MATERIALE PLASTICE
https://revmaterialeplastice.ro
https://doi.org/10.37358/Mat.Plast.1964

An Optimization Study on Material Selection for FRPCs in Multi Layered Armour System Through Hybrid MCDM Approach and Numerical Simulation

DARSHAN GOWDA[1], RAVISHANKAR BHAT[1], SANGAMESH RAJOLE[2]*
[1] Department of Metallurgical and Materials Engineering, National Institute of Technology Karnataka, Surathkal, Mangalore 575025, India
[2] Department of Mechanical Engineering, Central University of Karnataka, Kalaburgi 585367, India

Abstract: *Fiber reinforced polymer composites (FRPCs) are considered as core structure in Multi layered armour systems (MAS) to take advantage of maximum energy absorption, mobility and cost criteria design. In this article, based on the problem defining attribute's optimal material selection in FRPCs determined by Multiple criteria decisions making (MCDM) approach for considered alternative materials from polymer resin, synthetic and natural fiber. Attribute's weightage and alternatives priority rank were determined through Fussy-Analytical hierarchy process (F-AHP) and Technique for Order of Preference by Similarity to Ideal Solution (TOPSIS) method. Obtained rank was compared with Preference selection index (PSI) an another MCDM method, for better computational conformity. Selected materials from MCDM approach, simulated for energy absorption ability and damage after impact were studied by considering Cowper-Symonds constitutive materials model using 3D macro shell analysis. Various impact velocities were considered from 3 to 50 m/s for rigid steel impactor directed towards the deformable plate. Parameter like Residual kinetic energy, Residual velocity, Energy absorption ratio after impact were studied numerically. Simulation results in terms of specific energy absorption were compared with the rank obtained in MCDM approach. Among the polymers considered epoxy, polyurethane and polyester found better choice. In fibers hemp and basalt found better materials choice for heterogenous FRPCs design in ballistic armour.*

Keywords: *natural fiber, synthetic fiber, polymer matrix, MCDM approaches, ballistic impact*

1. Introduction

FRPCs find wide scope of application, due to its flexibility in design and adaptability. Some of the prominent application of FRPCs are aerospace, military, sport and leisure, food and packaging, transportation, civil construction, marine application etc. As like in other application, FRPCs considered in Multi layered armor system (MAS) most importantly to accomplish cost, weight and mobility criteria design objectives. In FRPCs, on the other hand, there was a demand for recyclable and eco-friendly materials due to societal concerns. Natural fibers considered as reinforcement in polymer matrix, have experience a renaissance [1–5]. Going by the present trends in research, due to regular revision in armor safety design requirements, and development of sophisticated weaponries. Dynamic safety and protection requirement for different engineering field, particularly in military application needed to be accomplish. Monolithic traditional metal and ceramic plates like steel, aluminum, titanium, boron caribe, silicon carbide and other metal oxides are inefficient for mobility criteria and cost-effective design [3]. These traditional plates have been largely replaced by low-weight, high-strength flexible fibers such as para-aramid (Kevlar), ultra-high-density polyethylene, glass, PBO (Zylon), M5 (PIPD), and carbon. Today's armor design is composed of several layers called "Multi Layered Armor System" (MAS) [2]. By simplifying its complex design, it has front specialized ballistic fiber stack followed by hexagonal ceramic plate and ductile back face signature as shown in Figure 1. Between these plates, soft core FRPCs with elastomer layers inserted for maximum energy absorption. Further followed by glass/phenolic laminate to get rid of toxic gases and hot bullet fragments.

**email: rajolesangmesh@gmail.com*

Ceramic plate purposed for destroys the high-speed bullet into fragments, it receives the initial compressive load and shock wave impedance generated by bullet impact and transit to FRPCs core further.

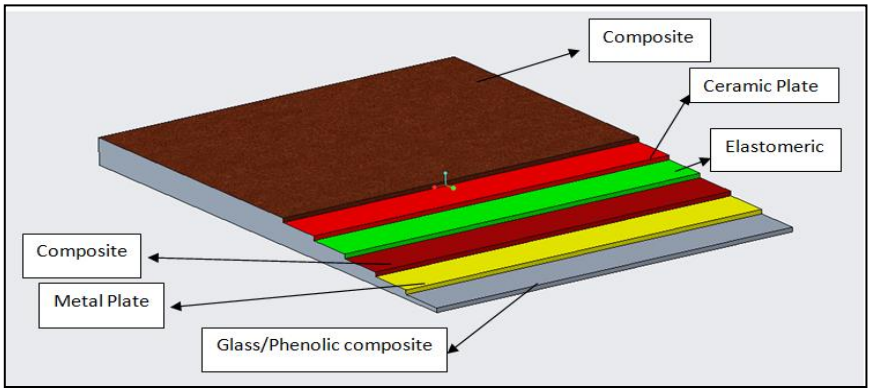

Figure 1. Typical multi-layered Armor system

Ceramic plate absorbs maximum kinetic energy of the bullet and responsible to damage it among the layers. Shock wave propagation in the ceramic was high than the FRPCs. At each interface partial tensile shock was reflected back. Since shock wave transit in solid was depends on density of the materials. At the interface of ceramic plate and FRPCs reflected tensile shock impedance was higher than the initial compressive impedance generated by bullet, it shatters the ceramic plate into fragments and it cause for the damage. Low density reinforcement in FRPCs like Kevlar, UHMPE and carbon etc. fiber will cause transmission and reflecting impedance shock pressure to be low at further layers. Further low-pressure shock waves reach the last ductile plate from FRPCs, and reflect the considerably low-pressure tensile shock impedance. Fibers in the FRPCs experience bending stretch by initial compressive shock, and partial relaxation by reflected tensile shock [2,3,6]. Due to this phenomenon, FRPCs failed by interlaminar shear and bucking effect. These phenomena make FRPCs to absorb and dissipate the energy of the bullet and its fragments efficiently in MAS.

Some of the researchers investigated the ballistic performance of hybrid FRPCs by considering front alumina ceramic plate and 5052 H34 aluminum plate as the back face signature. The experimental investigation reveals that the mechanical properties of FRPCs were enhanced by the hybridization of natural and synthetic fiber [2,3]. By hybridization of fibers multiple properties can be attained, fiber which is week in one mechanical property can be overcome by another fiber reinforcement [7]. Researchers tested for ballistic performance of MAS through considering various combination of FRPCs core. Jambari et al. [8] investigated the performance of hybrid Kenaf/Kevlar core sandwich for ballistic hard armour application, by considering different stacks. Through the impact test, energy absorption and ballistic limits capability of hybrid and non-hybrid laminate combination are studied. Among the hybrid combination 30/70 ratio reinforced hybrid Kenaf/Kevlar fiber laminate found high energy absorption capability than the other hybrid combination, and by comparing with 100% Kevlar laminate which shows 28% lower ballistic performance. Cruz et al. [9] investigated the 30 wt.% reinforced giant bamboo/epoxy laminate for ballistic performance and compared the results with same wt.% reinforced Kevlar/epoxy laminate and also with pure epoxy plate. MAS was tested for multiple shot criteria, as per NIJ standard. The measured depth of penetration for bamboo/epoxy laminate was less compared to Kevlar reinforced laminate, due to bamboo fiber decohesion and pretend the bullet fragments to pass through more effectively. More overly areal density and cost of MAS was reduced by 4% and 31%, by including hybrid fiber combination. Luz et al. [10] in their investigation study by considering intermediate coir mantel/epoxy laminate in MAS, was tested for personal protection vest application. A comparative study was made in term of depth of penetration and found that coir reinforced laminate shows better performance than the pure epoxy and Kevlar/epoxy laminate for single shot criteria. Rohen et al. [11] considered 30vol% Sisal reinforced epoxy laminate in MAS, tested for multiple shot withstand

capability. And by considering sisal reinforced laminate as intermediate layer in MAS found 20% more efficient in ballistic performance than aramid laminate. And overall, 5% lower areal density and 31% in cost reduction was achieved by comparing to Kevlar laminate. Luz et al. [12] Investigated the 30 vol% continuously aligned pineapple fiber (PALF)/epoxy tested for level IIIA ballistic vest protection, by considering front Al_2O_3 ceramic plate. To take the advantage of cost reduction, back face signature was not considered. Instead of that, low cost two layers of PALF/epoxy laminate jointed with polyurethane adhesive coat was considered for study. They compared the results with commercially available 25mm thick Dyneema FRPCs and other previous literature who considered FRPCs in MAS. Dyneema base FRPCs ballistic limit was found less than the PALF/epoxy laminate. As likely, Wambua and others [13] investigated the ballistic performance of woven jute, hemp and flax fabric in polypropylene resin individually for ballistic hard armor application. By varying the mild steel plate thickness to 1.5mm at fount end, its effect was studied and kinetic energy absorption capability was compared with other considered sandwich. Ballistic limit of the composite laminate found increases with increasing thickness of plate and Kinetic energy absorption increases as initial velocity of impact increases. Due to high ductility and strength of mild steel plate, both side metal plated MAS shows excellent ballistic limit than the single sided laminate. Flax sandwich alone without metal plate performs better in terms of energy absorption. Jute sandwich shows least ballistic limit and energy absorption than the other considered fiber sandwich. Oliveira and other [14–16] investigated various reinforced laminate, among them 40 vol.% fabric composites with fique fiber were found better alternative to aramid fibers. The additional advantage of low cost and fiber reinforcement favors back face signature deformation less than 44mm. Khodadadi et al. [17] On their investigation study of neat Kevlar fabric with hard/soft rubber matrices under high-velocity impact. The best performance was achieved by using Kevlar/hard rubber composite. By using hard rubber almost double increasing in ballistic limit can be achieved when compared to stiff polymer composites. Along with this experimental study, Finite element (FE) simulation packages like ABAQUS, DYNA3D, LSDYNA, ANSYS etc. was considered by the researcher for experimental results validation. Numerical and analytical methods increasingly often used by researchers to predict the properties of complex composite structures like woven fabric, Honey comb core and 3D printed cellular structures before fabrication [1,4,18–22]. Overall, Hybrid natural/synthetic fiber laminate suggested for mobility, cost and ecofriendly objective armor design.

It was found that from past many years researcher relayed on the statistical tool for the selection of materials. Designers and engineers have considered numerous attributes as decision-criteria for evaluating a material for their design [23,24]. In petrochemical industries due to excessive use of compressor to run the plant in various sections, need long term run without breakdown. Integrated F-AHP and F-TOPSSIS technique are followed to select most eligible compressors based on the required main criteria. Closeness co-efficient was determined to measure the efficiency of results [25]. Light weight environmentally friendly materials are extensively used in automobile application, which contributes for good operational performance with less fuel consumption, high sustainability. The proposed entropy-weighted MAIRCA found less complicated mathematical analysis, capability to handle large number of alternatives and criteria effectively. It was found that among the alternative ultra-high strength steel was suitable materials for concerned application [26]. Patnaik et al. [27] Followed hybrid AHP-MOORA approaches is applied to evaluate the best composite design for Wear resistant and Structural application. Weight for different considered criteria's are initially found by AHP approaches, and MOORA method are used to rank the alternatives. Among the combination 30 wt.% 400 GSM viscose fabric mat + 15 wt.% blast furnace slag + 55 wt.% epoxy found suitable for concerned application. Al-Oqla et al. [28] followed AHP MCDM method was used to evaluate the suitable natural fiber in automobile application. Based on the considered fibers like coir, date palm, flax, hemp and sisal. Flax fibers found most suitable based on the criteria of design, along with that some other potential fibers also have reasonable importance. Most researchers followed, Hybrid MCDM techniques to optimize the results and to rank the best alternatives with more accuracy. In most application researcher found MCDM was realistic and process optimization technique for product design. Since, individual MCDM technique

was different in their methodology and hybrid MCDM approach was followed to obtain better computational conformity.

In previous study researchers considered various FRPCs in MAS, based on its ballistic performance like energy absorption, its ballistic limit capability. Various fibers i.e., both natural and synthetic and various polymer matrix was considered to be potential materials for FRPCs design in MAS. Rather than considering monolithic metal plates, Synthetic/natural hybridized FRPCs laminate was preferred because it dissipates kinetic energy of the bullet and ceramic fragment through interface de-bonding, matrix crack and propagation with fiber damage more effectively. Researchers considering natural fiber in MAS, because of its unexpected ballistic performance like capture of ceramic and bullet fragment with excessive fiber decohesion without wedging. Material selection for FRPCs by considering multiple criteria and alternatives is challenging. For conceptual design of MAS, researchers rarely considered hybrid MCDM approach for materials selection. In this paper we followed hybrid MCDM technique like FUZZY-AHP-TOPSIS and PSI approaches for conceptual materials selection. And followed by macro shell FE simulation study for selected materials to drawn certain conclusion on its ballistic performance among them.

2. Materials and methods

2.1. Problem defining criteria's

In FRPCs damages like fiber shear breakage, delamination was the most common failure restrict to extensive impact loading application [5]. The performance of FRPCs under dynamic loading was of particular research interest, and this led to efforts to improve such properties. Four key parameters, namely fiber orientation geometry and stacking sequence, loading event, and environmental-related conditions, affect the structural behavior of FRPCs to impact loading [21]. As composite structures define the properties of finally fabricated laminate. The intrinsic system parameters such as ballistic material properties including fabric property (fabric type, weave design, fabric density), fibers and yarns properties and fabric finishing properties are considered. The extrinsic parameters such as ballistic impact methodology, ballistic target compositions and arrangement, ballistic target conditions, projectile type are considered for design. These properties which largely affects the ballistic impact performance of FRPCs [29]. Four main attributes like directional deformation, energy absorption, maximum stress and weight considered for armor design and followed grey relation analysis for ranking the best stack order. These parameters considered as per the NIJ standard 0101.02. Composite panel with maximum stress and energy absorption with minimum weight and deformation considered to be best [30]. Bullet parameters like size, shape, velocity and degree of hit are the important parameter to be considered for armor design. This property influenced on type of deformation made by bullet on the target, failure types, depth of perforation and area of perforation differs for different composite materials. These parameters were studied for UHDPE stack of 10,20 and 30mm thick laminate. Experimental results found that average energy absorption co-efficient increases with thickness. And shows different ballistic performance for different geometry of bullet [31].

Since, the areal density of the armour was reduced exponentially by replacing monolithic metal plate armour by MAS. Without compromising on its ballistic performance. Social, economic and environmental perspectives like low density, cost and biodegradability are the important factors for armour design to be considered [32]. Based on the above literature few problems defining criteria like cost, density, recyclability, tensile strength, tensile modulus, compressive strength, glass transition temperature and impact strength considered for polymer matrix selection. Criteria like cost, density, biodegradability, tensile strength and modulus considered for synthetic fiber selection and for natural fiber properties like tensile modulus, strength, elongation at break, density, microfibril angle, aspect ratio, moisture absorption, cellulose crystallinity, and cost are considered. In natural fibers cellulose is the main constituent. Its wt.%, crystallinity and helical angle of orientation define the mechanical properties [33]. All physical and economical attributes and its relative importance was considered as

lower value will be the better choice. All the attributes considered related to mechanical properties having higher value will be the better choice, which was shown in the Figure 2.

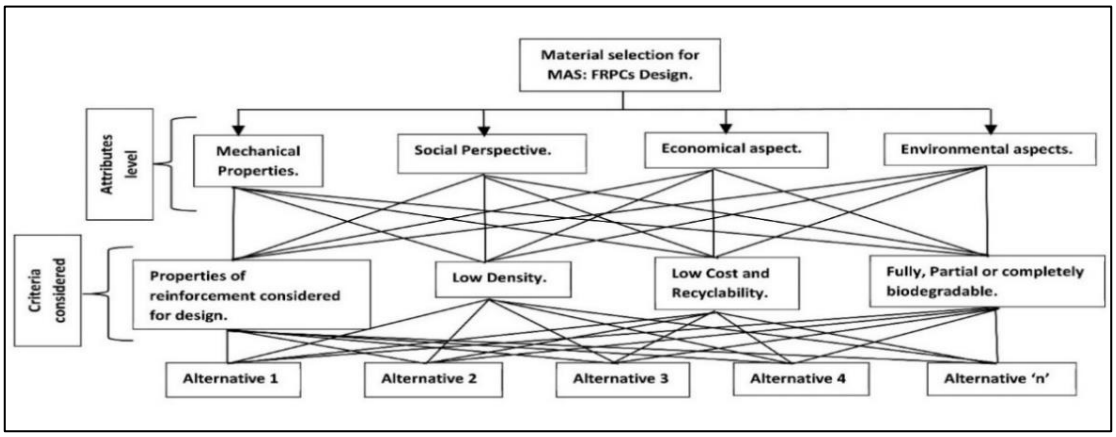

Figure 2. Problem defining criteria for ranking material for design

These positive/negative design criteria are evaluated by hybrid MCDM method among the alternatives considered. The decision matrix for polymer matrix, synthetic and natural fiber selection through MCDM approach is considered from the Table 1,2 and 3.

Table 1. Physical, ecnomical and mechnaical properties considered for Polymer marix selection through MCDM

Resin material	Cost/(USD.kg^{-1})	Density (g.cm^{-3})	Recyclability	Tensile Strength (MPa)	Tensile Modulus (GPa)	Compressive Strength (MPa)	Glass transition temperature.	Energy absorption or Izod impact(notched)(J/m)	References
PP	1	0.91	3	34.5	1.345	46.33	-10	27	[33-35]
PS	1.92	1.05	3	45	2.84	95	110	19.7	
Epoxy	6.41	1.6	1	60	4.00	135	100	45.00	
PVC	1.15	1.38	3	53	3.275	72	85	70	
Polyester	1.92	1.25	1	47	3.25	150	69	30	
Polycarbonate	3.5	1.2	3	62	2.38	86.1	141	8	
HDPE	1.26	0.99	3	25	1.1	22	-125	120	
Vinylester	4.62	1.4	1	86	3.8	60	114	20	
Phenolic	2.56	1.3	1	62	5	280	130	110	
PU	10.25	1.175	3	45	2.5	68.9	140	69.3	
Rubber	0.9	0.92	3	26	0.05	175	-72	70	

Table 2. Physical, ecnomical and mechnaical properties considered for Synthetic fibre

Fiber	Cost/(USD.kg^{-1})	Density (g/cm^3)	Non-biodegradable or Biodegradable	Tensile Strength (GPa)	Young's Modulus (GPa)	References
E- Glass	1.3	2.63	1	3.5	68.5	[36,37]
S- Glass	7	2.48	1	4.4	90	
Carbon	45	1.8	1	4	230	
P-aramid	3.55	1.47	1	3.5	179	
m-aramid	3.55	1.4	1	0.7	17	
UHMWPE	14	0.97	1	3.6	116	
Zylon AS	20	1.54	1	5.8	180	
Zylon HM	20	1.56	1	5.8	270	
Vectran	2	1.47	1	3.2	91	
M5	5	1.7	1	4	310	
Boron	1.3	2.64	3	3.85	430	
SiC	1.45	2.8	3	4	420	
AluminaIII	30	2.5	3	1.7	152	
Basalt	2.5	2.6	3	4.8	110	

Table 3. Physical, ecnomical and mechnaical properties considered for Natural fibre

Fiber materials	Tensile strength (MPa)	Tensile modulus (GPa)	Elongation at break (%)	Density (g/cm^3)	MFA (Degree)	Aspect ratio	Moisture content in plant	Cellulose crystallinity	Cost/ ($USD.kg^{-1}$)	References
Coir	175	4.50	33	1.3	40	35	10	30	1.25	[33,38–43]
Flax	690	27.6	3.1	1.49	8.00	1737	7	70	1.5	
Jute	480	19.75	2.3	1.23	8.00	100	12	70	0.35	
Hemp	845	70	3.05	1.35	6	1000	9	70	1.2	
Kenaf	612	53	4.8	1.2	8	238	10	60	1.3	
Ramie	669	94.7	3.00	1.44	8	4000	9	64	2	
Sisal	696	10.5	2.45	1.2	15.00	150	11	60	0.36	
Pineapple	898	58.5	2.00	1.2	14.00	150	13	52	0.05	
Banana	721	8.50	6.50	1.35	11.00	200	10.5	50	0.1	
Cotton	437	8.95	7.50	1.55	30	1250	7	50	1.85	
Oil palm	248	3.2	14	1.3	46	30.00	3.43	25	0.135	
Bamboo	695	20.50	2	1.2	7.00	193	8.9	50	1.77	

2.2. Materials selection by MCDM technique

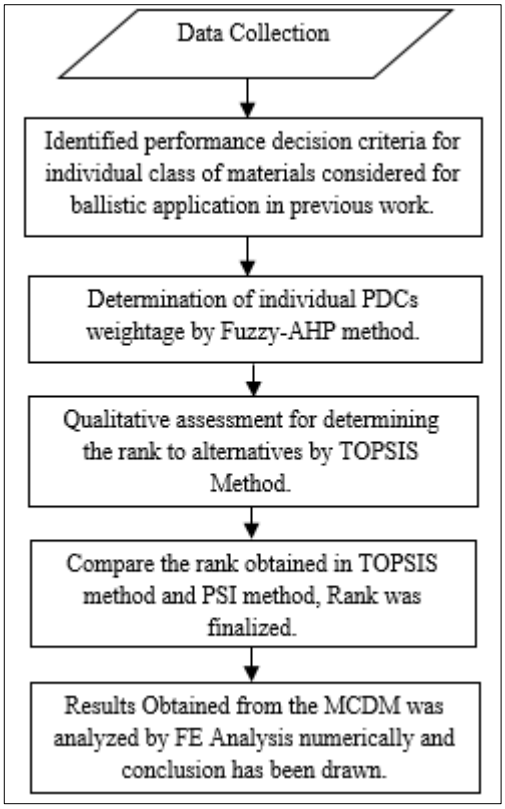

Figure 3. Methodology followed for materials selection from collected data was as followed

Based on the PDCs, alternatives materials considered for FRPCs design in MAS are evaluated. Hybrid MCDM i.e., Fuzzy-AHP and TOPSIS approaches was followed to select the optimal materials from respective categories. For better computational conformity obtained rank was compared with other MCDM technique i.e., PSI. The overall flow chart form conceptual material selection through MCDM to FE analysis was shown in the Figure 3.

2.3. Steps followed in Fuzzy-AHP method

For different materials selection in composites, the problem defining criteria (PDCs) were considered. To determine the weightage of considered PDCs for material selection. We followed extended FUZZY-AHP Method proposed by Chang [44,45].

Step 1: The AHP scale of relative importance, depicted in Figure 4, was assigned to pairwise relative comparisons with each other considered criterion. Relative importance was assigned numerically based on their significance. Here in our study, mechanical properties were considered as more importance's than physical, economical perspective. i.e., More weightage was given to mechanical properties. Decision matrix considered from Table 1, 2 and 3 above. From the decision matrix let, R = {R, R_2, R_3……R_n} be the criteria and S = {S_1, S_2, S_3……. S_m} be the alternative materials considered.

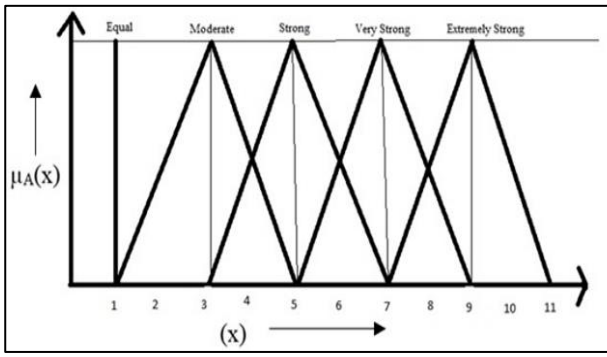

AHP scale	Linguistic term	Triangular Fuzzy number scale
1	Equal	(1,1,1)
3	Moderate	(2,3,4)
5	Strong	(4,5,6)
7	Very strong	(6,7,8)
9	Extremely strong	(9,9,9)
2		(1,2,3)
4	Intermediate values	(3,4,5)
6		(5,6,7)
8		(7,8,9)

Figure 4. Fuzzy scale of relative importance

Step 2: All assigned relative importance in AHP scale was converted into triangular fuzzy number shown in the Table 4,5 and 6. Which Symbolize the same linguistic meaning as like in AHP scale. The decision matrix comprises of criteria or alternatives in linguistic terms shown in Figure 4. The corresponding triangular fuzzy number indicates that it has a similar linguistic meaning to the AHP number. For example, "if criterion 1 (R_1) very strongly important than criterion 2 (R_2)", then it takes the fuzzy triangular number as (6,7,8). On the contrary, in the pair wise comparison matrix of the criteria, comparison of R_2 to R_1 was considered as reciprocal triangular fuzzy number as (1/8,1/7,1/6) [44]. The pair wise comparison matrix, by taking equal importance along the diagonal and reflecting its reciprocal value below its diagonal was shown below.

$$A=\begin{bmatrix} \mu_{11} & \cdots & \mu_{1n} \\ \vdots & \ddots & \vdots \\ \mu_{n1} & \cdots & \mu_{nn} \end{bmatrix}$$

The fuzzy pairwise comparison judgement were represented by fuzzy triangular number i.e., $\mu_{ij}(q)$ = (h, k, l), where subscript of 'μ' represents preference of i_{th} criteria over j_{th} criteria of q^{th} decision makers. The middle number in fuzzy triangular number, i.e., 'k' represents AHP scale of relative importance [44]. The converted Fuzzy-AHP matrix for synthetic and natural fiber, polymer resin shown in the Table 4,5 and 6.

Step 3: By the fuzzified pair-wise comparison matrix, the geometric mean value (M_i) was calculated [44]. It was represented by the equation (1).

$$M_i = \left(\prod_{j=1}^{n} \mu_{ij}(x)\right)^{1/n}, \; i = 1, 2, 3, \ldots..,n \tag{1}$$

The summation of reciprocal fuzzy geometric mean value multiplied with each fuzzy geometric mean value (M_i) of criteria given by the equation (2). On solving this equation, we obtain fuzzy weight (w_j) for each defined criteria's.

$$w_j = M_i * (M_1 + M_2 + M_3 + \cdots + M_n)^{-1} = (w_1, w_2, w_3) \tag{2}$$

where j = {1, 2……. n}

Step 4: De-Fuzzification was done by center of area (COA) method proposed by Chang [44], by the Equation (3).

$$\text{COA} = \frac{W_j = (w_1 + w_2 + w_3)}{3} \quad (3)$$

AHP scale of relative importance converted to fuzzy triangular number for pair wise comparison to find weightage for individual criteria. Middle value in fuzzy triangular number specifies the AHP scale of relative importance. Weights are normalized by dividing individual weight by total weight, to get sum of total normalized weight approximately equal to unity [44]. Normalized weight column shown in the Table 4,5 and 6. Finally, we obtain crisp numerical weights for individual criteria considered. These obtained weightages are further used for qualitative assessment for determining the priority rank in TOPSIS approach.

Table 4. AHP-Fuzzy Method followed to find normalized weight for synthetic fiber selection

Synthetic fiber	Cost	Density	Biodegradable or non-biodegradable	Tensile strength	Tensile modulus	Fuzzy geometric mean (M_j)	Fuzzy weight (w_j)	Weight. (COA)	Normalized weight
Cost	(1,1,1)	(0.33,0.5,1)	(0.2, 0.25, 0.33)	(0.16, 0.2, 0.25)	(0.16, 0.2, 0.25)	(0.28, 0.34, 0.46)	(0.03, 0.05, 0.10)	0.0648	0.06
Density	(1, 2, 3)	(1, 1, 1)	(2, 3,4)	(0.33, 0.5, 1)	(0.33, 0.5, 1)	(0.74, 1.08, 1.64)	(0.09, 0.17, 0.35)	0.21066	0.193
Biodegradable or non-biodegradable	(3, 4, 5)	(0.25, 0.33, 0.5)	(1, 1, 1)	(0.25, 0.33, 0.5)	(0.25, 0.33, 0.5)	(0.54, 0.68, 0.91)	(0.07, 0.11, 0.19)	0.1268	0.1162
Tensile strength	(4, 5, 6)	(1, 2, 3)	(2, 3, 4)	(1, 1, 1)	(1, 1, 1)	(1.51, 1.97, 2.35)	(0.19, 0.32, 0.51)	0.3444	0.3156
Tensile modulus(E)	(4, 5, 6)	(1, 2, 3)	(2, 3, 4)	(1, 1, 1)	(1, 1, 1)	(1.51, 1.97, 2.35)	(0.19, 0.32, 0.51)	0.3444	0.3156

Table 5. AHP-Fuzzy Method followed to find normalized weight for natural fiber selection

Natural fiber	Tensile strength	Tensile modulus	Elongation @break	Density	Micro fibril angle	Aspect ratio	Moisture	Cellulose crystallinity	Cost	Fuzzy geometric Mean (M_j)	Fuzzy weight (W_j)	Weight. (COA)	Normalized weight
Tensile strength	(1, 1, 1)	(1, 1, 1)	(1, 2, 3)	(4, 5, 6)	(2, 3, 4)	(1, 2, 3)	(5, 6, 7)	(1, 2, 3)	(2, 3, 4)	(1.62, 2.34, 2.97)	(0.10,0.20, 0.37)	0.229	0.1991
Tensile modulus	(1, 1, 1)	(1, 1, 1)	(1, 2, 3)	(4, 5, 6)	(2, 3, 4)	(1, 2, 3)	(5, 6, 7)	(1, 2, 3)	(2, 3, 4)	(1.62, 2.34, 2.97)	(0.10, 0.20, 0.37)	0.229	0.1991
Elongation @break	(0.33, 0.5, 1)	(0.33, 0.5, 1)	(1, 1, 1)	(3,4, 5)	(2, 3, 4)	(1, 2, 3)	(5, 6, 7)	(1, 2, 3)	(2, 3, 4)	(1.23, 1.81, 2.57)	(0.08, 0.16, 0.32)	0.1883	0.1637
Density	(0.16, 0.2, 0.25)	(0.16, 0.2, 0.25)	(0.2, 0.25, 0.33)	(1, 1, 1)	(0.33, 0.5, 1)	(0.33, 0.5, 1)	(5, 6, 7)	(0.33, 0.5, 1)	(1, 2, 3)	(0.46, 0.62, 0.91)	(0.03, 0.05,0.11)	0.0667	0.058
Micro fibril angle	(0.25, 0.33, 0.5)	(0.25, 0.33, 0.5)	(0.25, 0.33, 0.5)	(1, 2, 3)	(1, 1, 1)	(1, 2, 3)	(5, 6, 7)	(1, 1, 1)	(2, 3, 4)	(0.81, 1.11, 1.46)	(0.05, 0.09, 0.18)	0.112	0.097
Aspect ratio	(0.33, 0.5, 1)	(0.33, 0.5, 1)	(0.33, 0.5, 1)	(1, 2, 3)	(0.33, 0.5, 1)	(1, 1, 1)	(5, 6, 7)	(1, 2, 3)	(3, 4, 5)	(0.82, 1.22, 1.89)	(0.05, 0.10,0.23)	0.1333	0.116
Moisture	(0.14, 0.16, 0.2)	(0.14, 0.16, 0.2)	(0.14, 0.16, 0.2)	(0.14, 0.16, 0.2)	(0.14, 0.16, 0.2)	(0.14, 0.16, 0.2)	(1, 1, 1)	(0.16, 0.2, 0.25)	(0.33, 0.5, 1)	(0.19, 0.23, 0.29)	(0.01, 0.02,0.03)	0.0234	0.02
Cellulose crystallinity	(0.33, 0.5, 1)	(0.33, 0.5, 1)	(0.33, 0.5, 1)	(1, 2, 3)	(1, 1, 1)	(0.33, 0.5, 1)	(4, 5, 6)	(1, 1, 1)	(4, 5, 6)	(0.83, 1.13, 1.68)	(0.05, 0.10, 0.21)	0.122	0.106
Cost	(0.25, 0.33, 0.5)	(0.25, 0.33, 0.5)	(0.25, 0.33, 0.5)	(0.33, 0.5, 1)	(0.25, 0.33, 0.5)	(0.2, 0.25, 0.33)	(1, 2, 3)	(0.16, 0.2, 0.25)	(1, 1, 1)	(0.32, 0.43, 0.62)	(0.02, 0.03, 0.07)	0.0464	0.04

Table 6. AHP-Fuzzy Method followed to find normalized weight for polymer resin selection

Polymer resin	Cost	Density	Recyclability	Tensile strength	Tensile modulus	Compressive strength	Shear modulus	Impact strength	Fuzzy geometric mean (M_i)	Fuzzy weight(W_j)	Weight. (COA)	Normalized weight
Cost	(1, 1, 1)	(0.25, 0.33, 0.5)	(2, 3, 4)	(0.16, 0.2, 0.25)	(0.16, 0.2, 0.25)	(0.16, 0.2, 0.25)	(0.16, 0.2, 0.25)	(0.16, 0.2, 0.25)	(0.29, 0.36, 0.45)	(0.02, 0.03, 0.05)	0.0379	0.0361
Density	(2, 3, 4)	(1, 1, 1)	(1, 2, 3)	(0.16, 0.2, 0.25)	(0.16, 0.2, 0.25)	(0.2, 0.25, 0.33)	(0.2, 0.25, 0.33)	(0.16, 0.2, 0.25)	(0.37, 0.48, 0.61)	(0.03, 0.04, 0.07)	0.05	0.0476
Recyclability	(0.25, 0.33, 0.5)	(0.33, 0.5, 1)	(1, 1, 1)	(0.16, 0.2, 0.25)	(0.16, 0.2, 0.25)	(0.16, 0.2, 0.25)	(0.16, 0.2, 0.25)	(0.16, 0.2, 0.25)	(0.23, 0.29, 0.38)	(0.01, 0.02, 0.04)	0.0309	0.0294
Tensile Strength	(4, 5, 6)	(4, 5, 6)	(4, 5, 6)	(1, 1, 1)	(1, 1, 1)	(1, 2, 3)	(1, 2, 3)	(1, 1, 1)	(1.68, 2.17, 2.57)	(0.13, 0.21, 0.30)	0.2171	0.207
Tensile Modulus(E)	(4, 5, 6)	(4, 5, 6)	(4, 5, 6)	(1, 1, 1)	(1, 1, 1)	(1, 1, 1)	(1, 2, 3)	(1, 1, 1)	(1.68, 1.99, 2.24)	(0.13, 0.19, 0.26)	0.1985	0.1893
Compressive Strength	(4, 5, 6)	(3, 4, 5)	(4, 5, 6)	(0.33, 0.5, 1)	(1, 1, 1)	(1, 1, 1)	(1, 1, 1)	(1, 1, 1)	(1.41, 1.63, 1.91)	(0.11, 0.15, 0.22)	0.1664	0.1587
Shear Modulus(G)	(4, 5, 6)	(3, 4, 5)	(4, 5, 6)	(0.33, 0.5, 1)	(0.33, 0.5, 1)	(1, 1, 1)	(1, 1, 1)	(0.33, 0.5, 1)	(1.07, 1.37, 1.91)	(0.08, 0.13, 0.22)	0.149	0.1421
Impact Strength	(4, 5, 6)	(4, 5, 6)	(4, 5, 6)	(1, 1, 1)	(1, 1, 1)	(1, 1, 1)	(1, 2, 3)	(1, 1, 1)	(1.68, 1.99, 2.24)	(0.13, 0.19,0.26)	0.1985	0.1893

2.4. Steps followed in TOPSIS method

Technique for the Order of Preference by Similarity to Ideal Solution (TOPSIS) most followed MADM method in many applications, for selecting the matrix and reinforcement phase in composite. TOPSIS scale of measure were defined as 1 value signifies low, 2 value signifies below average, 3 value signifies average, 4 value signifies good and 5 value signifies excellent. This scale was considered for non-numerical attributes like biodegradable/non-biodegradable and recyclability criteria. The step involved in TOPSIS method as follows [46,47]:

Step 1: Problem definition: Attributes considered from defined objectives, governing equation and from the past research in the previous case study are evaluated by Fuzzy-AHP method, to find weightage of these attributes considered. Weightage assigned by Fuzzy-AHP method was considered in TOPSIS approach to sort best alternative among them, by assigning rank.

Step 2: Calculate the normalized matrix, from the given equation (4).

$$N_{ij} = \frac{z_{ij}}{\sqrt{\sum_{j=1}^{n} z_{ij}^2}} \quad (4)$$

Step 3: TOPSIS matrix was formulated based on the decision matrix Table 1,2 and 3 shown below:

$$Q = \begin{bmatrix} Z_{11} & \cdots & Z_{1n} \\ \vdots & \ddots & \vdots \\ Z_{m1} & \cdots & Z_{mn} \end{bmatrix}$$

Let S_1, S_2……. S_m are the different alternative considered along the column and R_1, R_2……. R_n are criteria or attributes considered along the rows. Z_{ij} is the rating of alternatives S_i with respect to attributes R_j.

Step 4: Calculate weighted normalized matrix, with the help of weight concluded from the Fuzzy-AHP method. It was given by the Table 7,8 and 9. It was given by the equation (5).

$$D_{ij} = N_{ij} * W_j \quad (5)$$

where $\sum W_j = 1$;

Step 5: Calculate the ideal best and ideal worst values by the equation (6) and (7), where A_1 corresponds to benefit criteria and A_2 corresponds to cost criteria.

$$D_j^+ = \{(\max D_{ij}, a \in A_1), (\min D_{ij}, a \in A_2), i = 1,2,3\ldots., m\} \ \forall \ a \quad (6)$$

$$D_j^- = \{(\min D_{ij}, a \in A_1), (\max D_{ij}, a \in A_2), i = 1,2,3\ldots., m\} \ \forall\ a \quad (7)$$

Step 6: Calculate the distances o_i^+ and o_i^- from the positive ideal and negative ideal solutions from the Equation (8) and (9).

$$o_i^+ = \{\sum_{j=1}^{n}(D_{ij} - D_j^+)^2\}^{1/2}\ ;\ \forall\ i \quad (8)$$

$$o_i^- = \{\sum_{j=1}^{n}(D_{ij} - D_j^-)^2\}^{1/2}\ ;\ \forall\ i \quad (9)$$

Step 7: Determine relative closeness (r_i^+) of alternatives to the ideal solution, from the Equation (10). Alternatives with higher magnitude of closeness are preferred. Its value given in the Table 7, 8 and 9.

$$r_i^+ = \frac{o_i^-}{o_i^+ + o_i^-}\ ;\ \forall\ i, \text{ where } 0 \le r_i^+ \le 1 \quad (10)$$

Table 7. TOPSIS normalized decision matrix for synthetic fiber

Fibre	Cost	Density	Non-biodegradable or Biodegradable	Tensile Strength	Young's Modulus	Relative closeness (r_i^+)	Rank obtained by Fuzzy-AHP and TOPSIS
E- Glass	0.0205	0.3423	0.1474	0.2341	0.0809	0.3281	12
S- Glass	0.1102	0.3227	0.1474	0.2943	0.1062	0.3929	10
Carbon	0.7083	0.2343	0.1474	0.2675	0.2715	0.5167	6
P-aramid	0.0559	0.1913	0.1474	0.2341	0.2113	0.4700	7
m-aramid	0.0559	0.1822	0.1474	0.0468	0.0201	0.2158	14
UHMWPE	0.2204	0.1262	0.1474	0.2408	0.1369	0.4069	9
Zylon AS	0.3148	0.2004	0.1474	0.3879	0.2125	0.5603	5
Zylon HM	0.3148	0.2030	0.1474	0.3879	0.3187	0.6716	3
Vectran	0.0315	0.1913	0.1474	0.2140	0.1074	0.3580	11
M5	0.0787	0.2212	0.1474	0.2675	0.3659	0.6615	4
Boron	0.0205	0.3436	0.4423	0.2575	0.5076	0.7497	1
SiC	0.0228	0.3644	0.4423	0.2675	0.4958	0.7443	2
Alumina III	0.4722	0.3253	0.4423	0.1137	0.1794	0.3172	13
Basalt	0.0394	0.3384	0.4423	0.3210	0.1298	0.4562	8

Table 8. TOPSIS normalized decision matrix for natural fiber

Fibre materials	Tensile strength	Tensile modulus	Elongation at break (%)	Density	MFA	Aspect ratio	Moisture content in plant	Cellulose crystallinity	Cost	Relative closeness (r_i^+)	Rank obtained by Fuzzy-AHP and TOPSIS
Coir	0.0797	0.0304	0.8655	0.2837	0.5394	0.0075	0.3022	0.1545	0.2964	0.4240	3
Flax	0.3143	0.1862	0.0813	0.3252	0.1079	0.3723	0.2115	0.3604	0.3557	0.3227	6
Jute	0.2186	0.1333	0.0603	0.2684	0.1079	0.0214	0.3626	0.3604	0.0830	0.2526	9
Hemp	0.3849	0.4723	0.0800	0.2946	0.0809	0.2143	0.2720	0.3604	0.2846	0.4360	2
Kenaf	0.2788	0.3576	0.1259	0.2619	0.1079	0.0510	0.3022	0.3089	0.3083	0.3575	5
Ramie	0.3047	0.6390	0.0787	0.3143	0.1079	0.8573	0.2720	0.3295	0.4743	0.5734	1
Sisal	0.3170	0.0708	0.0643	0.2619	0.2023	0.0321	0.3324	0.3089	0.0854	0.2497	10
Pineapple	0.4091	0.3947	0.0525	0.2619	0.1888	0.0321	0.3928	0.2677	0.0119	0.3833	4
Banana	0.3284	0.0574	0.1705	0.2946	0.1483	0.0429	0.3173	0.2574	0.0237	0.2765	7
Cotton	0.1991	0.0604	0.1967	0.3383	0.4046	0.2679	0.2115	0.2574	0.4387	0.2025	11
Oil palm	0.1130	0.0216	0.3672	0.2837	0.6203	0.0064	0.1036	0.1287	0.0320	0.2166	12
Bamboo	0.3166	0.1383	0.0525	0.2619	0.0944	0.0414	0.2689	0.2574	0.4198	0.2739	8

Table 9. TOPSIS normalized decision matrix for polymer resin

Polymer matrix	Cost	Density ($g.cm^{-3}$)	Recyclable	Tensile strength (MPa)	Tensile modulus (GPa)	Compressive strength (MPa)	Glass transition temperature	Energy absorption or Izod impact(notched)(J/m) (ASTM D-256)	Relative closeness (r_i^+)	Rank obtained by Fuzzy-AHP and TOPSIS
PP	0.0710	0.2256	0.3665	0.1984	0.1347	0.1085	-0.0284	0.1264	0.3187	9
PS	0.1363	0.2603	0.3665	0.2588	0.2844	0.2225	0.3119	0.0922	0.3044	10
Epoxy	0.4551	0.3967	0.1222	0.3450	0.4005	0.3161	0.2836	0.2107	0.4394	4
PVC	0.0816	0.3422	0.3665	0.3048	0.3279	0.1686	0.2410	0.3277	0.4203	5
Polyester	0.1363	0.3099	0.1222	0.2703	0.3254	0.3513	0.1957	0.1405	0.4038	6
Polycarbonate	0.2485	0.2975	0.3665	0.3565	0.2383	0.2016	0.3998	0.0375	0.2686	11
HDPE	0.0895	0.2470	0.3665	0.1438	0.1101	0.0515	-0.3544	0.5618	0.5144	2

Vinyl ester	0.3280	0.3471	0.1222	0.4945	0.3805	0.1405	0.3233	0.0936	0.4009	7
Phenolic	0.1818	0.3223	0.1222	0.3565	0.5007	0.6557	0.3686	0.5150	0.6112	1
PU	0.7277	0.2913	0.3665	0.2588	0.2503	0.1615	0.3970	0.3249	0.3310	8
Rubber	0.0639	0.2281	0.3665	0.1495	0.0050	0.4098	-0.2042	0.3277	0.4724	3

2.5. Steps followed in PSI method

Step 1: Criteria and alternatives defined in the early steps from the formulated decision matrix in Fuzzy-AHP method i.e., from the Table 1,2 and 3. Same decision matrix was considered for determining the best alternative among them in PSI approach [48].

Step 2: Find a Normalized matrix: The process of transforming the decision matrix attributes value into compactible scale ranges from 0-1 value is called "normalization". Criteria considered in decision matrix as both types i.e., non-beneficial and beneficial. If it is beneficial one then larger the value is better and if it is non-beneficial then smaller the value is better. Then the attributes performance can be found by equation (11) and (12).

$$P_{ij} = \frac{Z_{ij}}{Z_j^{max}} \tag{11}$$

$$P_{ij} = \frac{Z_j^{min}}{Z_{ij}} \tag{12}$$

where, Z_{ij} is the attributes measures for i = {1, 2, 3...n} and j = {1, 2, 3…m}.

Step 3: The average of the normalized attribute value was calculated from the equation (13), where 'a' is the number of alternatives.

$$A = \frac{1}{a}\sum_{i=1}^{a} Z_{ij} \tag{13}$$

Find the preference of variation for individual criteria. It can be calculated by taking square of difference between normalized value and mean of normalized value, takes its average for each criteria. It can be calculated from equation (14).

$$V_j = \sum_{i=1}^{n}\left(Z_{ij} - A\right)^2 \tag{14}$$

Step 4: Calculate the deviation of preference value for each attribute can be found by equation (15).

$$d = [1 - V_j] \tag{15}$$

The overall preference weight was determined for individual criteria from the equation (16). The overall preference value for all criteria equal to one, $\sum_{j=1} \theta_j$.

$$O_j = \frac{\theta_j}{\sum_{j=1}^{n} \theta_j} \tag{16}$$

Step 5: Find the PSI (I_i) by computing with individual alternative from the equation (17).

$$I_i = \sum_{j=1}^{n} Z_{ij} * O_j \tag{17}$$

Step 6: Rank the alternative based on the highest value obtained in I_I value for Individuals. The normalized decision matrix calculated for polymer resin, synthetic and natural fiber selection was shown in the Table 10,11 and 12.

Rank obtained in Fuzzy-AHP-TOPSIS and PSI approach are consolidated and given in the Table 7-12. Obtained priority rank was having considerable difference, which can be verified. Finally, rank was

concluded based on the nearest rank obtained from the both methods. It was found that among the natural and synthetic fiber hemp, flax, ramie and basalt, para-aramid, M5 was found best alternative for armor design. Among the polymer resin considered epoxy, Polyurethane and polyester resin was found best alternative through conceptual design. In synthetic fiber even though boron, silicon carbide and Nextel fiber was preferred top order in MCDM approaches. These fiber materials are considered as front plates in MAS than in fiber form in most investigations [49]. So, subsequent rank materials such as basalt, para-aramid, M5 was considered for FE analysis.

Table 10. Normalized decision matrix for synthetic resin selection obtained from PSI approach

Fibre	Cost	Density	Non-biodegradable or Biodegradable	Tensile Strength	Young's Modulus	PSI (I_i)	Rank obtained by PSI
E- Glass	1.000	0.369	0.333	0.603	0.159	1.601	3
S- Glass	0.186	0.391	0.333	0.759	0.209	-0.677	10
Carbon	0.029	0.539	0.333	0.690	0.535	-1.140	11
P-aramid	0.366	0.660	0.333	0.603	0.416	-0.490	8
m-aramid	0.366	0.693	0.333	0.121	0.040	-0.245	7
UHMWPE	0.093	1.000	0.333	0.621	0.270	-1.982	14
Zylon AS	0.065	0.630	0.333	1.000	0.419	-1.620	13
Zylon HM	0.065	0.622	0.333	1.000	0.628	-1.495	12
Vectran	0.650	0.660	0.333	0.552	0.212	0.188	5
M5	0.260	0.571	0.333	0.690	0.721	-0.513	9
Boron	1.000	0.367	1.000	0.664	1.000	2.645	1
SiC	0.897	0.346	1.000	0.690	0.977	2.382	2
Alumina III	0.043	0.388	1.000	0.293	0.353	0.194	6
Basalt	0.520	0.373	1.000	0.828	0.256	0.837	4

Table 11. Normalized decision matrix for natural fiber selection obtained from PSI approach

Natural Fibre	Tensile strength	Tensile Modulus	Aspect Ratio	Cellulose crystallinity	Elongation at break	Density	MFA	Moisture content	Cost	PSI (I_i)	Rank obtained by PSI
Coir	0.195	0.048	0.006	0.429	1	0.923	0.15	0.343	0.04	0.580	12
Flax	0.768	0.291	0.29	1	0.064	0.87	0.75	0.49	0.033	0.719	1
Jute	0.535	0.209	0.017	1	0.07	0.976	0.75	0.286	0.143	0.676	7
Hemp	0.941	0.739	0.167	1	0.092	0.889	1	0.381	0.042	0.707	2
Kenaf	0.682	0.56	0.04	0.857	0.145	1	0.75	0.343	0.038	0.678	5
Ramie	0.745	1	1	0.914	0.091	0.833	0.75	0.381	0.025	0.669	8
Sisal	0.775	0.111	0.025	0.857	0.074	1	0.4	0.312	0.139	0.691	3
Pineapple	1	0.618	0.025	0.743	0.061	0.8	0.429	0.264	1	0.612	10
Bannana	0.803	0.09	0.033	0.714	0.197	0.889	0.545	0.327	0.5	0.652	9
Cotton	0.487	0.095	0.208	0.714	0.227	0.774	0.2	0.49	0.027	0.602	11
Oil plam	0.276	0.034	0.005	0.357	0.424	0.923	0.13	1	0.037	0.677	6
Bamboo	0.774	0.216	0.032	0.714	0.061	1	0.857	0.385	0.028	0.681	4

Table 12. Normalized decision matrix for polymeric resin selection obtained from PSI approach

Polymer matrix	Cost	Density	Recyclable	Tensile strength	Tensile modulus	Compressive strength	Glass transition temperature	Energy absorption or Izod impact	PSI (I_i)	Rank obtained by PSI
PP	0.9	1	1	0.401163	0.269	0.165464	-0.07092	0.225	-0.879	9
PS	0.46875	0.866667	1	0.523256	0.568	0.339286	0.780142	0.164167	0.994	4
Epoxy	0.140406	0.56875	0.333333	0.697674	0.8	0.482143	0.70922	0.375	0.800	6
PVC	0.782609	0.65942	1	0.616279	0.655	0.257143	0.602837	0.583333	0.676	7
Polyester	0.46875	0.728	0.333333	0.546512	0.65	0.535714	0.489362	0.25	0.284	8
Polycarbonate	0.257143	0.758333	1	0.72093	0.476	0.3075	1	0.066667	1.493	2
HDPE	0.714286	0.913655	1	0.290698	0.22	0.078571	-0.88652	1	-2.620	11
Vinylester	0.194805	0.65	0.333333	1	0.76	0.214286	0.808511	0.166667	0.925	5
Phenolic	0.351563	0.7	0.333333	0.72093	1	1	0.921986	0.916667	1.044	3
PU	0.087805	0.774468	1	0.523256	0.5	0.246241	0.992908	0.578269	1.550	1
Rubber	1	0.98913	1	0.302326	0.01	0.625	-0.51064	0.583333	-1.905	10

2.6. Numerical analysis

Even though Carbon fiber reinforced composite are superior in specific modulus and strength, it was prone to delamination failure and underperforms for low impact application was concluded through numerical approach. The study was caried for 2D and 3D woven fabrics in epoxy resin of different laminate thickness of 6.35 and 25.4 mm. Experimental and computational results was compared, it reveals that both the results in terms of ballistic limits was found the same [50]. On experimental validation of JE(Jute-epoxy) sandwich after projectile hit the target clear perforation with brittle fracture indicates not support for high velocity impact. In JRE(Jute-rubber-epoxy) sandwich after projectile hit, the middle rubber core supports the ductile fracture with high absorption of energy. On increasing the thickness from 3 to 15 mm the energy absorption increased by 80% were achieved. This type of experimental results has been validated and compared by considering various damage model like Hashin anisotropic model, Johnson-cook (JC) plasticity model etc. in ABAQUS and other FE packages [51,52]. As like other damage model, few researchers considered Cowper–Symonds elasto-plastic model to evaluate the dynamic properties by considering coupled effect of strain and strain rate. For moderate strain rate of 10^4 per second, this materials model was largely considered for explicit analysis study [53,54]. The analysis for kinetic energy absorption capability of plate impacted by bullet was analyzed by commercially available LS-Dyna. The target plate of shell type was designed as per ASTM D 7136, and a bullet of sphere shape rigid solid was considered for study. The bullet was drifted at three velocities range from low, intermediate and high, i.e, 3, 30 and 50 m/s perpendicular to the plate in Z-direction. The 3D deformable shell Plate of dimension 150x100x5 mm^3 was fixed at its extremities considered for study. Steel sphere bullet of mass 15.90 g was considered [49,55]. The assemble was shown in the Figures 5 and 6. The meshing details was given in the Table 13.

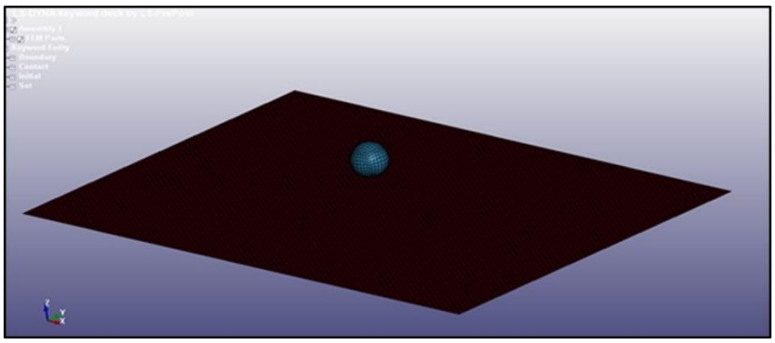

Figure 5. Assembly of bullet and plate

Plate and bullets set as automatic surface to surface contact with static friction coefficient of 0.2 and damping coefficient of 0.1 was considered. For a designed 3D shell plate and 3D rigid steel impactor, materials properties were defined through MAT003- Plastic kinematics and MAT020-Rigid solid option [56]. Element failure after impact was analyzed by Cowper-Symonds constitutive materials model without considering stain rate effect. The flow stress was given below [53].

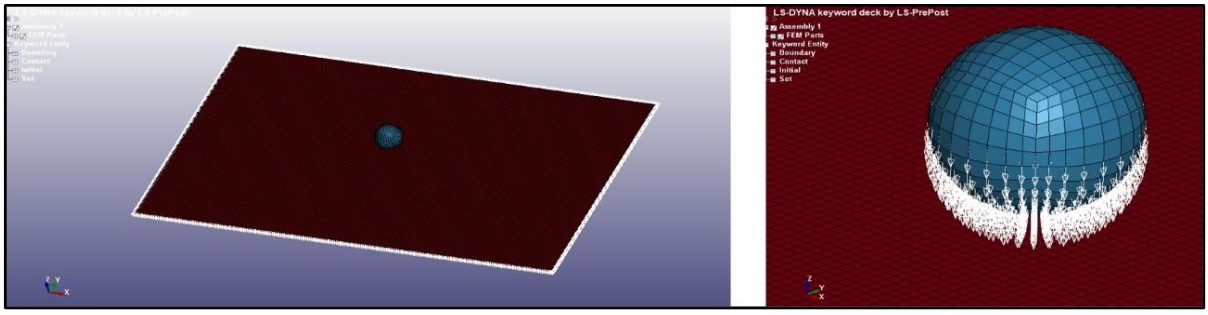

Figure 6. Boundary condition for plate fixed at the boundaries and bullet projection at Z-direction was shown

$$\sigma_{flow} = ((\sigma_0 + \beta * \frac{E_t.E}{E-E_t} * \varepsilon_{ff}^p) * (1 + \frac{\epsilon}{C})^{\frac{1}{P}} + (E_t * \varepsilon_{ff}^p)) \quad (18)$$

Here from the above equation (18), we considered the kinematic hardening i.e., β = 0. Strain rate effect ($\in$) was excluded, so dynamic yield stress was equal to static yield stress. The above flow stress Equation was reduced to equation (19) [53]; where σ_0= Static yield stress, E_t= Tangential modulus at yield static stress and ε_{ff}^p= Effective plastic strain.

$$\sigma_{flow} = ((\sigma_0 + (E_t * \varepsilon_{ff}^p)) \quad (19)$$

Theoretically calculated tangential modulus from the equation (20), its values for individual materials tabulated in the Table 14 considered for simulation study.

$$E_t = \frac{(\text{Ultimate true stress} - \text{Yileld true stress})}{(\text{Ultimate true strain} - \frac{\text{Ultimate true stress}}{\text{Elastic modulus}})} \quad (20)$$

2.7. Equations considered for impact performance evaluation are given below [57–60]

Final residual kinetic energy after impact was calculated from equation 22. Difference between initial and residual kinetic energy defines the total energy absorbed by the plate. Residual velocity of the bullet can be estimated from equation 23. Energy absorption ratio with respect to initial kinetic energy was calculated from equation 24.

Isotropic materials Equation: E = 2G(1+ν), E=3K(1-2ν) (21)

Energy Absorption (E^a) = Initial Kinetic energy(KE^I) – Residual Kinetic energy (KE^F)

$$= (\frac{1}{2}\, m * V_I^2 - \frac{1}{2}\, m * V_R^2) \quad (22)$$

Residual Velocity of bullet, $V_R = \sqrt{\frac{2KE^F}{m}}$ (23)

Energy Absorption Ratio, γ (%) = $\frac{E^a}{KE^I}$ (24)

Table 13. Meshing details of each part

Part Name	Type of element used	Material property type	Number of element/nodes
Plate	3D shell type Isotropic	MAT003-PLASTIC KINEMATICS	37500
Sphere Bullet	3D solid sphere Isotropic	MAT020-RIGID SOLID	5103

Top first three rank materials preferred through hybrid MCDM approach was considered for simulation study individually. Conclusion in terms of energy absorption ratio and element failure area after impact was analyzed and final choice has been made from the respective categories. Its individual material properties, considered from various reference were shown in the Table 14.

Table 14. Materials properties considered for FE simulation

Material		Weight Density (Kg/m^3)	Elastic modulus (GPa)	Poisson ratio	Yield strength (MPa)	Max Strain at failure or Max % Elongation	Bulk Modulus (GPa)	Shear modulus (GPa)	Calculated Tangential Modulus (E_t)	References
Polymer resin	PolyUrethane	1125	1.1	0.41	3.5	4.52	2.03	0.390	9.26	[1,33,41,42]
	Epoxy	1300	1.5	0.38	9.82	1.410	2.08	0.543	36.62	
	Phenolic	1300	1.378	0.31	13	0.65	1.20	0.526	80.99	

Synthetic fibre	Basalt	2640	110	0.22	3100	3.15	65.48	45.08	547.2	
	M5	1700	310	0.3	4300	2.5	258.3	119.2	16.08	
	P aramid	1450	109	0.36	3000	2	129.76	40.07	254.07	
Natural fibre	Hemp	1350	70	0.3	580	4.5	58.33	26.9	59.04	
	Flax	1380	27.5	0.3	343	3	22.91	10.57	116.64	
	Ramie	1440	94.7	0.3	400	4	78.91	36.42	67.368	

3. Results and discussions

By plotting the radar chart, comparison of rank obtained from both MCDM approach was made. Among the chosen material, which obtained best rank from the both MCDM approaches was considered for simulation study. The Consistency Ratio (CR) for considered relative important matrix to evaluation weightage through AHP method was found to be 0.054, 0.051, 0.037 for synthetic fiber, natural fiber and polymeric matrix. Which is less than 10%, and shows that considered relative importance values among the attributes for weightage evaluation in Fuzzy-AHP was in consistent [44]. To get clarity on MCDM results, a radar chart was plotted based on the rank obtained from both methods shown in Figure 7.

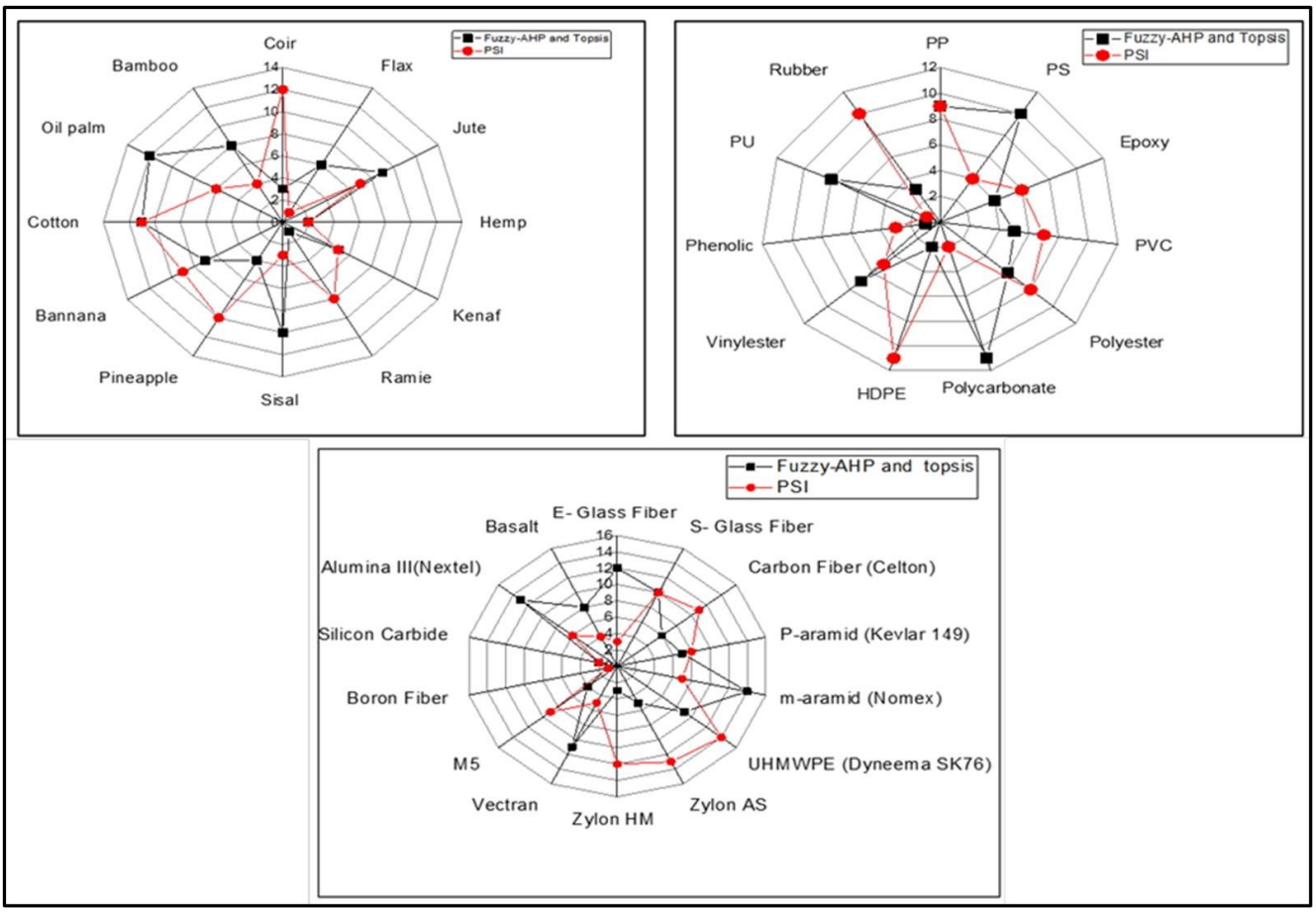

Figure 7. Radar chart for synthetic and natural fiber, polymer matrix based on the ranking obtained

Among the polymers Epoxy, phenolic and poly urethane resin was found best material for armor design. In synthetic fiber even though boron, silicon carbide and Nextel was preferred in top rank, these ceramic materials are largely considered as front in MAS than in fiber form. So, subsequent rank materials like basalt, M5 and P-aramid considered as top order priority and in natural fiber flax, hemp and ramie found as better choice. The explicit interaction of bullet with plate shown in the Figure 8.

Table 15 shows simulated results obtained numerically for different Impact velocity of bullet (m/s), parameter like Initial Kinetic Energy (J), Residual Kinetic Energy (J), Energy Absorbed (J), Residual velocity (m/s), Velocity Drop (m/s) and Energy Absorption Ratio, γ (%) are calculated by considering impact performance evaluation equations.

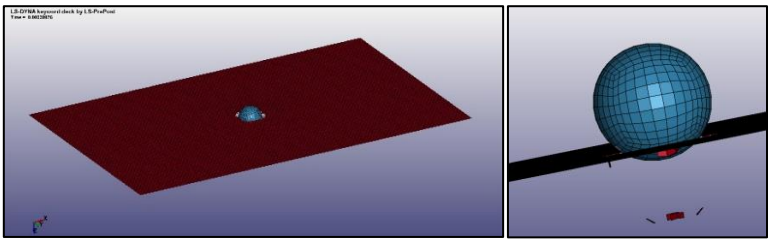

Figure 8. Brittle damage of epoxy plate impacted by bullet at 30m/s

Table 15. Simulation results

Material		Impact velocity of bullet (m/s)	Initial Kinetic Energy (J)	Residual Kinetic Energy (J)	Energy Absorbed (J)	Residual velocity (m/s)	Velocity Drop (m/s)	Energy Absorption Ratio, γ (%)	Types of Impact	Avg. overall Energy Absorption Ratio
Synthetic Resin	Epoxy	3	0.07	0.0057	0.064	0.85	2.15	91.86	Rebound	53.87
		30	7.043	3.6	3.44	21.28	8.72	48.89	Complete penetration	
		50	19.56	15.48	4.08	44.13	5.87	20.86		
	Phenolic	3	0.07	0.0058	0.064	0.85	2.15	91.71	Rebound	50.14
		30	7.043	4.36	2.68	23.42	6.58	38.09	Complete penetration	
		50	19.56	15.525	4.04	44.19	5.81	20.63		
	Polyurethane	3	0.07	0.0141	0.055	1.33	1.67	79.86	Rebound	47.38
		30	7.043	4.207	2.84	23	7	40.27	Complete penetration	
		50	19.56	15.253	4.31	43.8	6.2	22.02		
Natural Fibre	Flax	3	0.07	0.005576	0.064	0.837	2.163	92	Rebound	88.48
		30	7.043	0.80222	6.241	10.045	19.955	88.6		
		50	19.56	2.9716	16.588	19.334	30.666	84.8	Partial Damage	
	Hemp	3	0.07	0.004619	0.065	0.762	2.238	93.4	Rebound	90.3
		30	7.043	1.0251	6.018	11.355	18.645	85.4		
		50	19.56	1.5507	18.009	13.966	36.034	92	Partial Damage	
	Ramie	3	0.07	0.00518	0.065	0.807	2.193	92.6	Rebound	89.97
		30	7.043	0.94977	6.093	10.93	19.07	86.5		
		50	19.56	1.7963	17.764	15.032	34.968	90.8	Partial Damage	
Synthetic Fibre	M5	3	0.07	0.00672	0.063	0.919	2.081	90.4	Rebound	91.23
		30	7.043	0.4742	6.569	7.723	22.277	93.3		
		50	19.56	1.9611	17.599	15.706	34.294	90	Partial Damage	
	Basalt	3	0.07	0.01374	0.056	1.315	1.685	80.4	Rebound	91.66
		30	7.043	0.1724	6.871	4.657	25.343	97.6		
		50	19.56	0.5801	18.98	8.542	41.458	97	Partial Damage	
	P aramid	3	0.07	0.00346	0.067	0.66	2.34	95.1	Rebound	90.26
		30	7.043	0.952	6.091	10.943	19.057	86.5		
		50	19.56	2.1098	17.45	16.291	33.709	89.2	Partial Damage	

In this numerical study bullet drifted at different velocity regime from low to high, which impart different initial kinetic energy. Impact results like kinetic energy absorption ratio for selected materials form hybrid MCDM studied individually. At different velocity like low, moderate and high i.e., 3, 30 and 50 m/s given to impactor drifted perpendicular to the fixed target plate. Bullet impart 0.07, 7.043

and 19.56 J of initial kinetic energy. Variations of energy absorption ratio at different impact velocity for different materials shown by plotting bar chart in the Figure 9.

Based on the overall average energy absorption ratio at different impact velocity, materials deicide for armor design. Among the matrix materials considered, epoxy resin found better in average energy absorption ratio at all velocity regime. Among the synthetic fibers based on the average kinetic energy absorption ratio, Basalt fiber takes top priority order. Similarly, among the natural fiber Hemp was found in top priority order. Obtained order of priority almost resembled same order priority obtain in MCDM approaches, when compared with the simulation results in terms of average energy absorption ratio. It can be verified from the bar charts that for increasing initial velocity (Initial kinetic energy) i.e., from 3 to 50 m/s both synthetic and natural fibers show marginally increase in energy absorption except for polymer matrix, due its damage at 30 and 50 m/s velocity regime. So, final kinetic energy absorption depends on the initial velocity of the bullet. For different velocity impact energy absorption ratio was dominated by stiffness modulus and yield strength of materials.

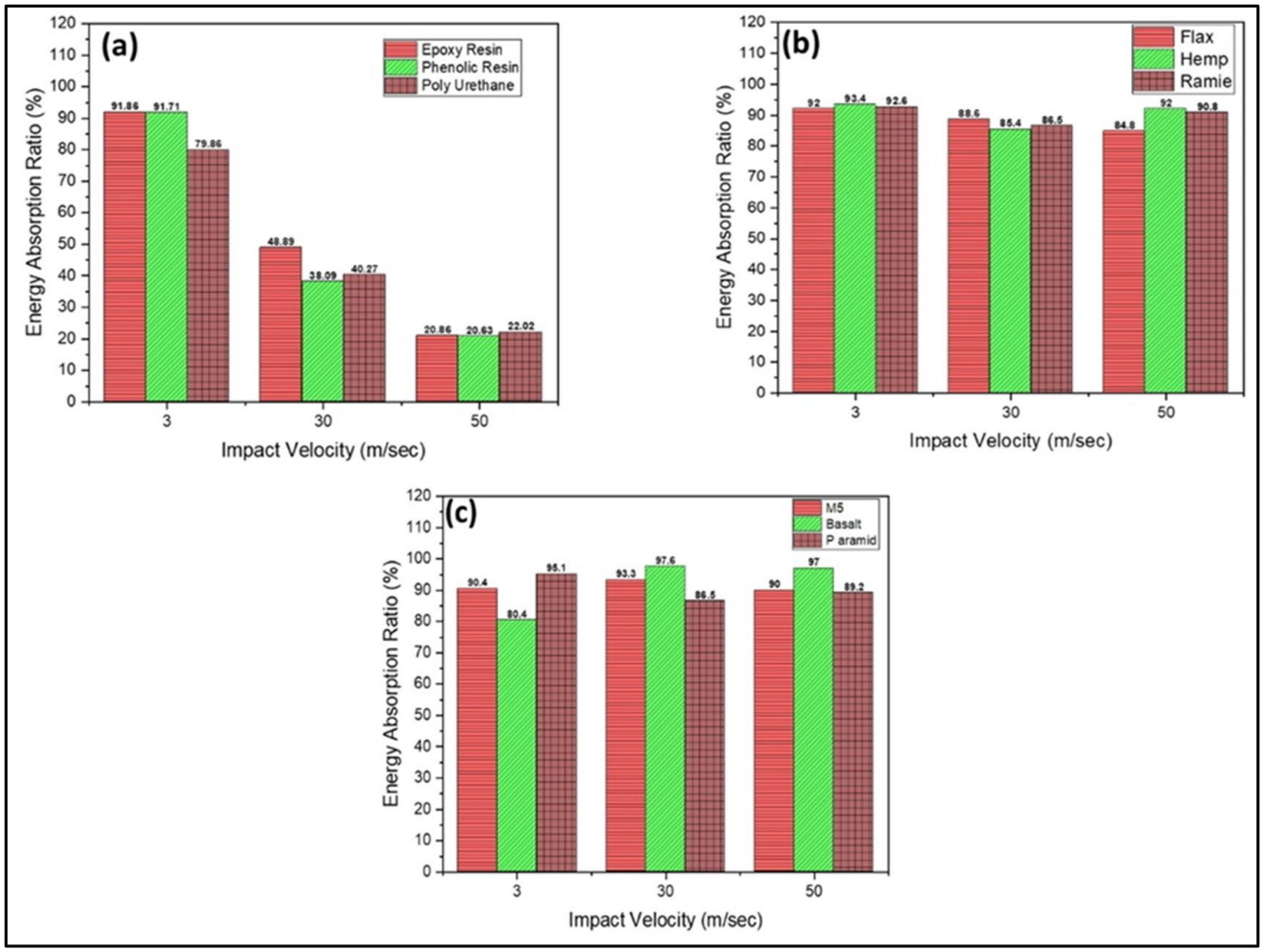

Figure 9. Variation of Energy absorption ratio (J) Vs Impact velocity of bullet (m/s)

Polymer plate failed by brittle crack for higher initial kinetic energy, epoxy have higher stiffness modulus than polyurethane which shows higher energy absorption considerably. The bar chart for energy absorption ratio for polymer materials, it shows decreasing trend for higher velocity impact at 30 and 50 m/s due to significant damage shown in Figure 9a. But overall average kinetic energy absorption ratio for resin was found better for epoxy resin at all velocity ranges. Unlike from polymer plate, fibers show no complete perforation after impact. Due to which there was marginally slight difference in energy absorption found, which can be verified from Figure 9b and c. Bullet will rebound back with

certain residual kinetic energy after impact. By comparing the overall average energy absorption ratio, synthetic basalt and natural hemp fiber was found the better in their respective categories. And overall trend for individual materials from each classes shows increasing energy absorption ratio except for resin. Mechanically Polymeric material having less strength than fibers got diminishing trend due to damage. By comparing the average energy absorption capability of synthetic basalt and natural hemp fiber, synthetic basalt fiber shows almost 1.51% higher average energy absorption than hemp fiber for overall velocity ranges. Among the synthetic fibers basalt fiber shows 1.55% higher than P-aramid fiber, in natural fiber hemp shows 2.06% higher energy absorption than flax fiber. Among the matrix material epoxy shows 11.98% higher energy absorption at moderate and high velocity regime than poly urethane resin, which can be justified from Table 15 and Figure 9.

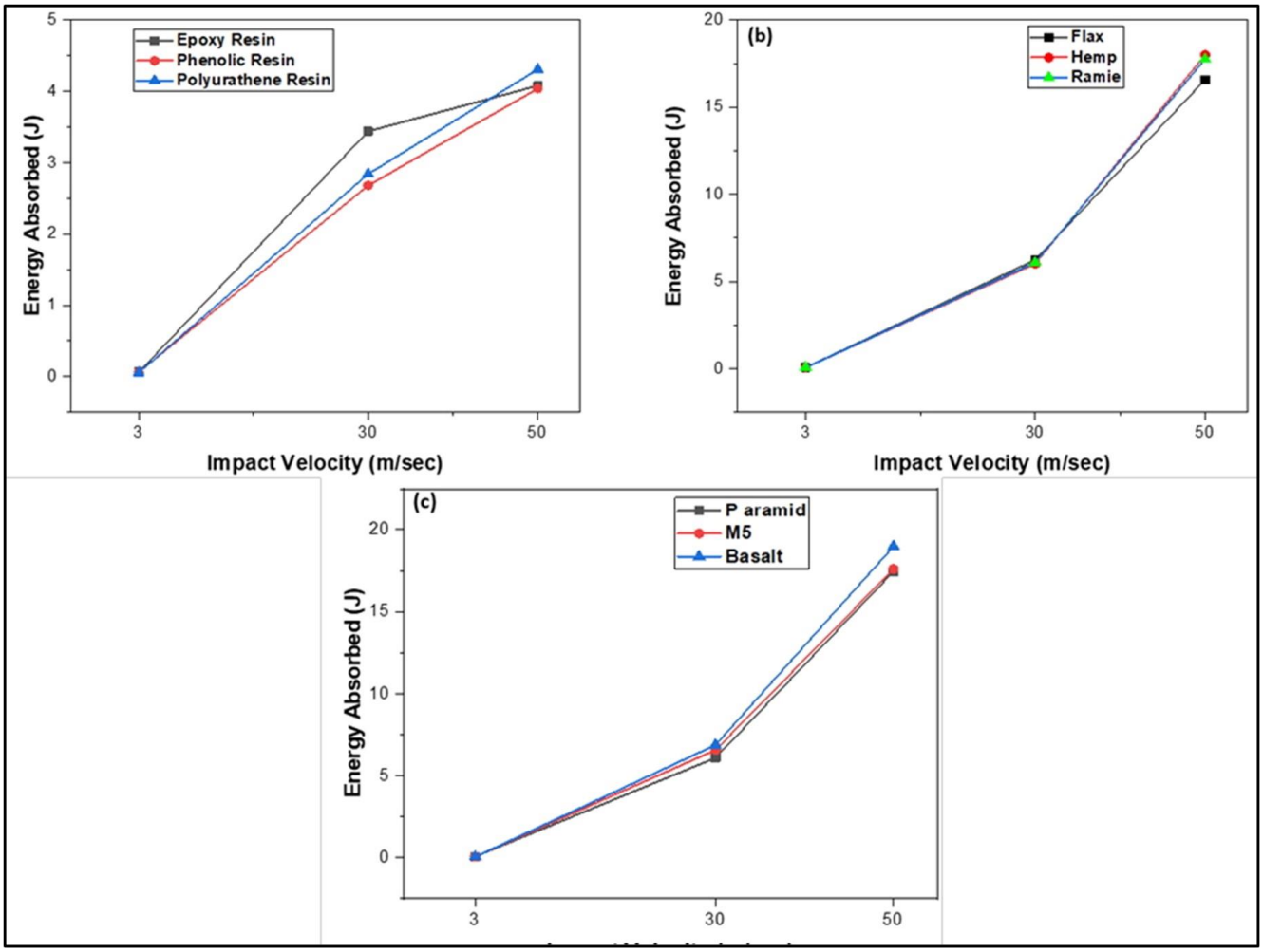

Figure 10. Plotted for Energy absorbed (J) Vs Impact velocity (m/s) variation

Variation of energy absorbed by the plate at different Impact velocity shown in the Figure 10. It was observed that, there was a considerable difference in energy absorption response shows among the materials. Among the resin Poly urethane exhibit superior elasticity at low impact velocity. Which shows higher rebound residual velocity with higher energy absorption, due to its high ductility. At moderate and higher velocity regime, the polymer target plate leads to perforation with brittle crack shown in the Figure 8. At this velocity regime epoxy exhibits superior energy absorption than phenolic and poly urethane resin due to higher stiffness modulus, which can be verified from the Table 15. As like in matrix materials, at all velocity regime basalt fiber and hemp fiber shows highest drop in velocity and better energy absorption than others fiber. It can be verified from the Figure 10b and 10c for fibers at different velocity impact and from Table 15. From the resultant displacement vs time graph, at 50 m/s initial

impact velocity of bullet. Polymer plate doesn't show any rebound as shown in Figure 11a, a linear tread shows complete perforation or damage. Area of damage was approximately calculated after impact at 50 m/s by drawing a circle. It shows that epoxy plate was damage with an area of 3.397 * 10^{-4} mm^2 which is 15.29% and 13.76% less damage area compared to phenolic and polyurethane resin shown in the Figure 12. For synthetic and natural fiber, at 50 m/s bullet rebound back with residual velocity which can be justified from the Figure 11b and c. Its velocity will drop to zero and again projected back with certain residual velocity, due to high fiber strength bullet unable to pass through. These drop in velocity was not found in polymer resin, because of complete damage and got linear trend.

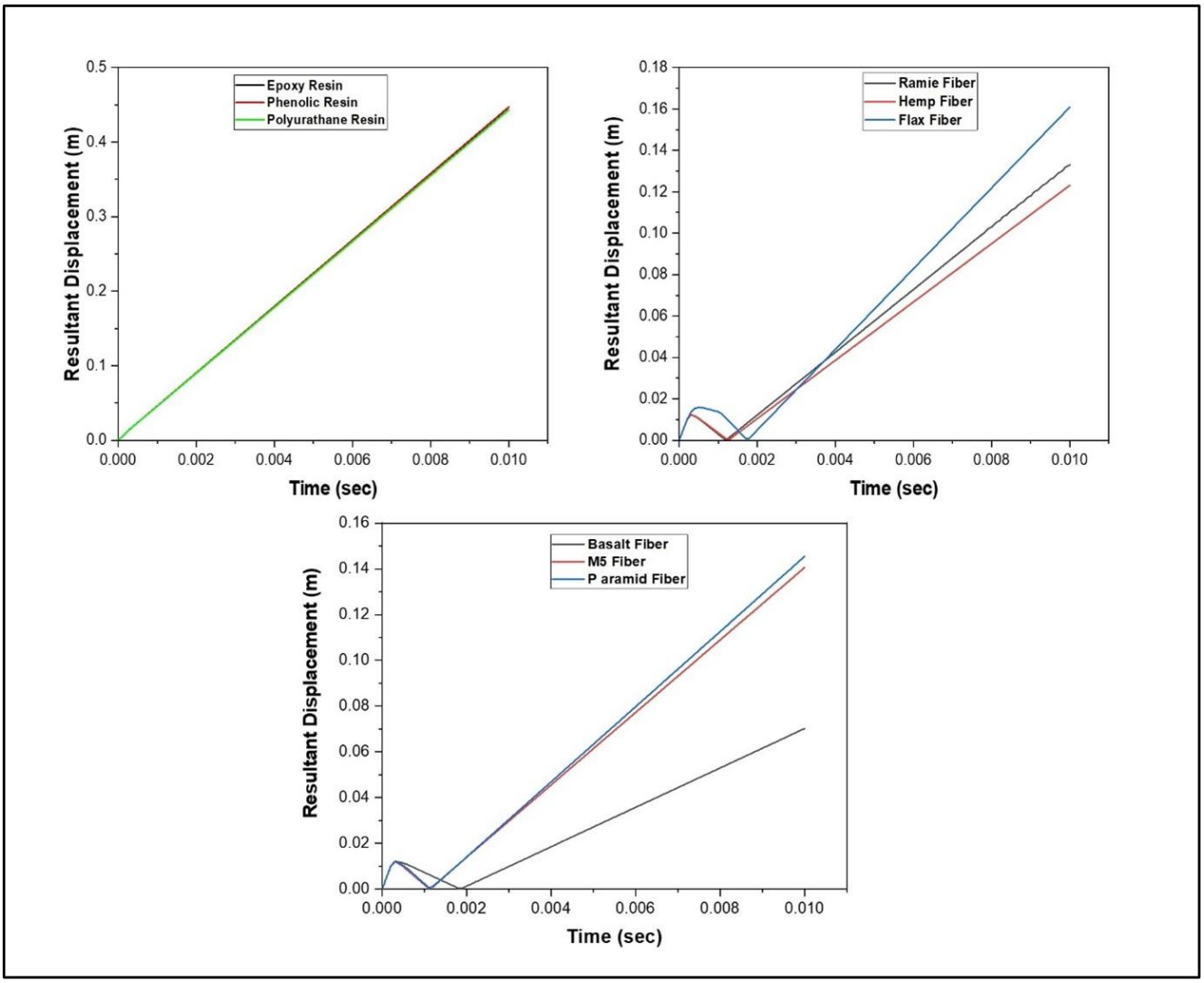

Figure 11. Variation resultant displacement with time, at impact velocity 50 m/s

The critical area of max von mises stress distribution was approximated for damaged plates, it was found that hemp and basalt fiber show least area of damage at the point of impact at 50 m/s. There was a localized impression/bulge projection was found for synthetic and natural fiber materials at the point of impact. From the impact point, stress distribute to its surroundings and its total maximum effected area was calculated by drawing circle as like in polymer, which was shown on the Figure 12. The maximum effective stress deformation by the materials depends on the yielding. Beyond the yielding point materials plastically deform and stretch upto the maximum failure strain and bullet will erode the plate. Area of effective von mises stress distribution at the point of impact shows high for phenolic resin and due to its high yield strength than the epoxy and poly urethane plate, it means area of damage was high for phenolic plate shown in the Figure 12. Among the fibers flax and P aramid was found higher

area of damage than other materials considered from the respective classes. Variation of difference in kinetic energy before and after impact shown in Figure 13. And variation of total energy absorbed by the plate and residual velocity of bullet was calculated from equation (22) and (23), and results are tabulated in the Table 15.

The kinetic energy of impactor reduces after it contact with the plate, during which internal energy of the plate increases. The kinetic energy of the bullet reaches minimum point, and internal energy of plate reaches to maximum value. Due to elasticity of plate at 3 m/s low velocity impact, bullet rebound back with certain residual velocity. The residual kinetic energy of the plate increases from the low point of rebound back position and become constant at later stages. This constant energy considered as residual kinetic energy of plate.

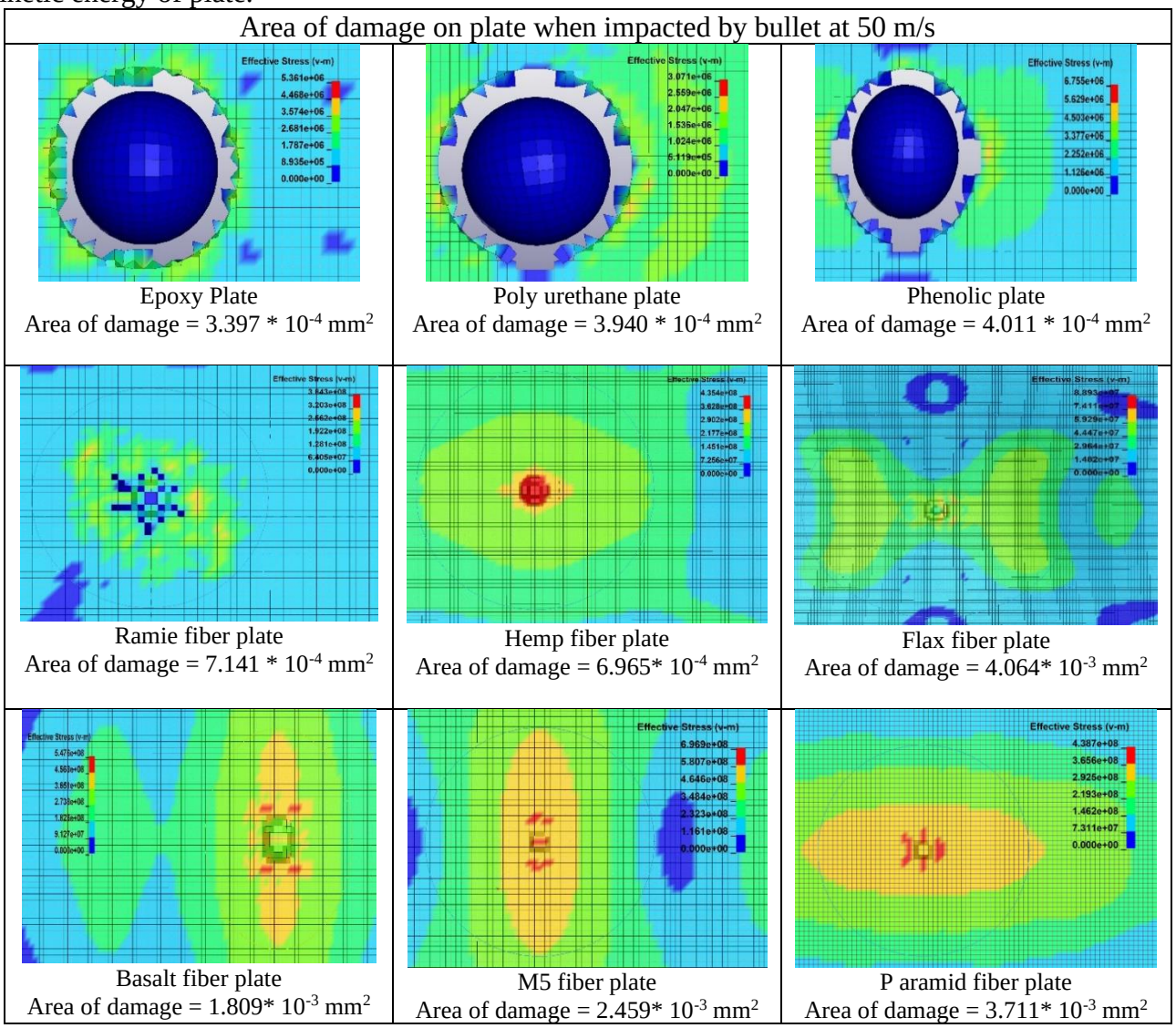

Figure 12. Area of damage evaluation at 50m/s for different plates

The total energy absorption difference calculated from equation (22). At 3 m/s velocity regimes the impactor will not penetrate the target resin plate. But for moderate and higher initial kinetic energy impact, there was no such sign of rebound back kinetic energy was found due to failure of the plate. It can be verified from the Figure 13b and c. Similarly, for fibers due to higher stiffness modulus impactor was failed to pass though target. Like in resin for low velocity impact, bullet will rebound back for all considered velocity impact for fibers. The synthetic fiber like Para-aramid and M5 considered for numerical simulation, developed specially for ballistic application. For ecofriendly and cost criteria armour design basalt fiber can be considered and has equivalent potential like other fibers. Through this

numerical analysis we can come to know that, there is no large difference in average overall energy absorption ratio among the natural and synthetic fibers was found. Natural fiber has potential reinforcement can be considered for ballistic application as individually or in hybrid form.\

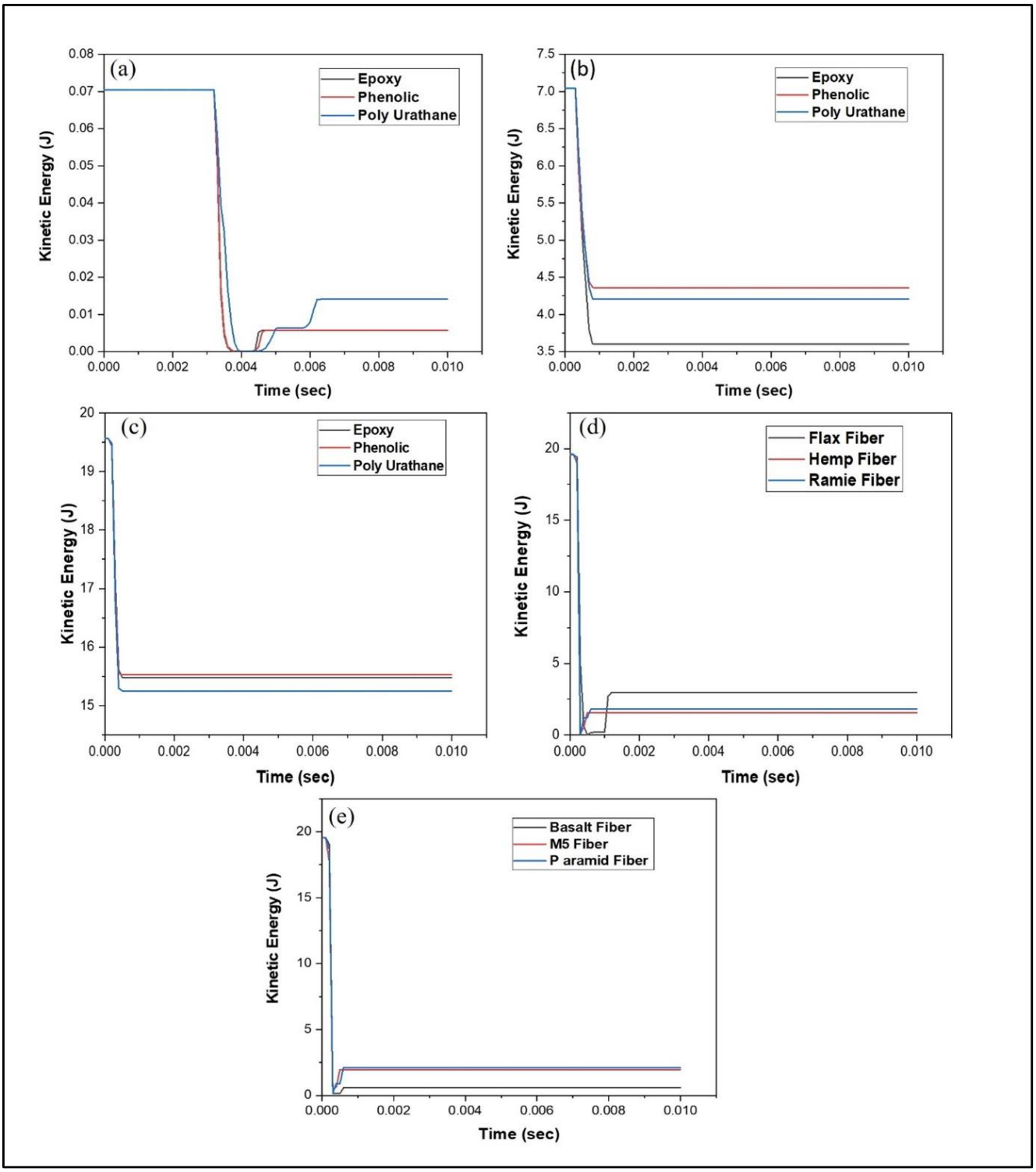

Figure 13. variation of kinetic energy Vs time at 3, 30 and 50 m/s velocity impact for resin shown in a, b and c, d, e show variation at 50 m/s for natural and synthetic fibers

Figure 14 shows effective stress distribution after impact. Since polymeric plate tends to fail by brittle crack at 30 and 50 m/s. At 3 m/s impactor rebound back with increasing kinetic energy from the low point. The effective rebound and perforation position of the bullet showed in Figure 14 a, b and c for

epoxy plate. The eroded fracture elements after reaching failure strain can be verified from Figure 8. Numerically it was found that, due to higher strain at failure of polyurethane. Plate undergoes larger deformation after impact.

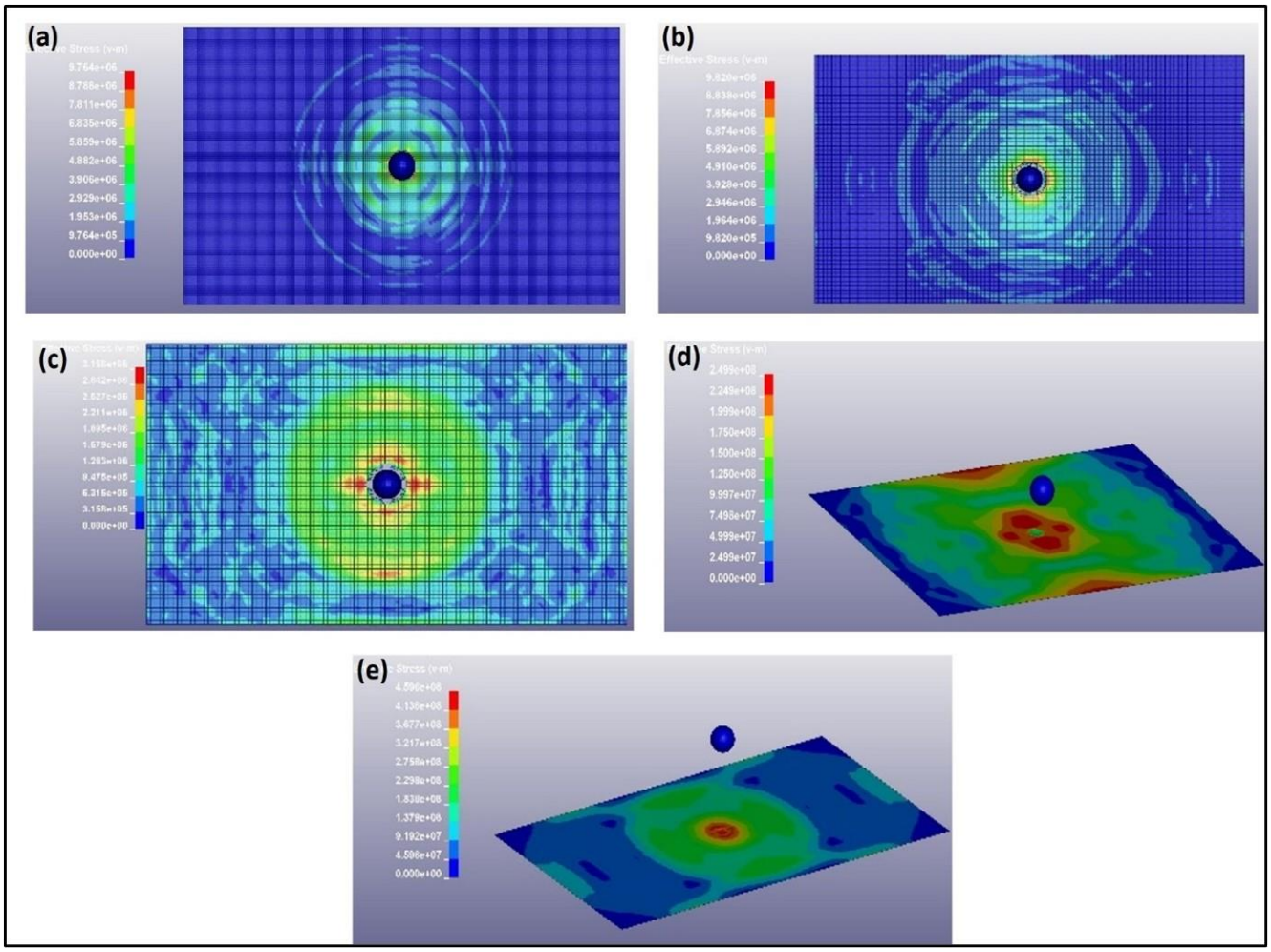

Figure 14. a, b and c on Von Mises Stress distribution for Epoxy plate impacted at 3, 30 and 50 m/s, d and e for hemp and basalt fiber plate impacted at 50 m/s

At low velocity impact significant drop in residual kinetic energy and velocity of impactor, with maximum energy absorption was found. For fibers at these velocity ranges no damage or perforation found. But point of impression made by bullet with deformation after impact can be identified. Since fiber possess high modulus properties compared to polymeric resin. Fibers have high capability to withstand the kinetic energy imparted by bullet than brittle polymers. The effective rebound position of bullet after impact at 50 m/s for hemp and basalt fiber shown in the Figure 14d and e.

4. Conclusions

Materials selection for FRPCs design in armour involved with multiple constraints and criteria to be considered. From the individual class of large alternative materials, it is challenging to select among the best materials for design. For cost, mobility and ecofriendly objective design of armour. Through Fussy-AHP-TOPSIS MCDM approach conceptual materials selection was made, and compare the results with other technique i.e, PSI for better computational conformity. And for selected materials ballistic performance was evaluated through macro shell numerical approach. From both MCDM and numerical study, it is concluded that:

- the rank obtained from the both MCDM approach was compared by plotting radar chart and its results found reasonable and consistent. Among the polymer matrix, it was found that epoxy, phenolic, and polyurethane were better material choices for the considered objectives. Among the synthetic fiber basalt, M5, and Para-aramid found to be better choices. As likely, among the natural fiber hemp, flax, and ramie found to be better choices for reinforcement in FRPCs. It was concluded through Hybrid MCDM conceptual design, these fiber reinforcement and polymer matrix materials can be considered for FRPCs design in MAS. Performance study has been made by considering Cowper-Symonds constitutive materials model through 3D shell macro analysis. It was found reasonable approach to consider Cowper-Symonds constitutive materials model for FE analysis for impact application;

- by contrasting the average overall energy absorption ratio at various velocity ranges. The performance of phenolic and polyurethane plates is reduced by 6.92 and 12.05%, respectively, when compared to epoxy. Flax has a 0.37% decrease in performance and ramie has a 2.02% decrease in performance when compared to natural hemp fiber. M5 and P aramid have lower performance than synthetic basalt fiber by 0.47 and 1.53%, respectively.

- based on the area of damage calculation after impact at 50 m/s. It was found that poly urethane plate shows 15.98% and phenolic plate shows 18.09% more area of damage than the epoxy plate. For the same velocity impact, among the synthetic and natural fibers. M5 and Ramie shows 35.93% and 2.53% more area of damage than the synthetic basalt and natural hemp fiber.

- based on the hybrid MCDM conceptual design for materials selection and numerical ballistic performance study. It was found that, obtained priority rank and numerically preferred best materials from both methods was comparable and consistent.

References

1. K.N. KEYA, N.A. KONA, F.A. KOLY, K.M. MARAZ, MD.N. ISLAM, R.A. KHAN, Natural fiber reinforced polymer composites: history, types, advantages, and applications, Materials Engineering Research. 1 (2019) 69–87. https://doi.org/10.25082/MER.2019.02.006.

2.N.M. NURAZZI, M.R.M. ASYRAF, A. KHALINA, N. ABDULLAH, H.A. AISYAH, S.A. RAFIQAH, F.A. SABARUDDIN, S.H. KAMARUDIN, M.N.F. NORRRAHIM, R.A. ILYAS, S.M. SAPUAN, A Review on Natural Fiber Reinforced Polymer Composite for Bullet Proof and Ballistic Applications, Polymers (Basel). 13 (2021) 646. https://doi.org/10.3390/polym13040646.

3.S.N. MONTEIRO, J.W. DRELICH, H.A.C. LOPERA, L.F.C. NASCIMENTO, F.S. DA LUZ, L.C. DA SILVA, J.L. DOS SANTOS, F. DA COSTA GARCIA FILHO, F.S. DE ASSIS, É.P. LIMA, A.C. PEREIRA, N.T. SIMONASSI, M.S. OLIVEIRA, L.C. DA CRUZ DEMOSTHENES, U.O. COSTA, R.H.M. REIS, W.B.A. BEZERRA, Natural Fibers Reinforced Polymer Composites Applied in Ballistic Multilayered Armor for Personal Protection-An Overview, in: 2019: pp. 33–47. https://doi.org/10.1007/978-3-030-10383-5_4.

4.F. TANASĂ, M. ZĂNOAGĂ, C. TEACĂ, M. NECHIFOR, A. SHAHZAD, Modified hemp fibers intended for fiber-reinforced polymer composites used in structural applications-A review. I. Methods of modification, Polymer Composites. 41 (2020) 5–31. https://doi.org/10.1002/pc.25354.

5.R. LATIF, S. WAKEEL, N. ZAMAN KHAN, A. NOOR SIDDIQUEE, S. LAL VERMA, Z. AKHTAR KHAN, Surface treatments of plant fibers and their effects on mechanical properties of fiber-reinforced composites: A review, Journal of Reinforced Plastics and Composites. 38 (2019) 15–30. https://doi.org/10.1177/0731684418802022.

6.S. MONTEIRO, A. PEREIRA, C. FERREIRA, É. PEREIRA JÚNIOR, R. WEBER, F. ASSIS, Performance of PlainWoven Jute Fabric-Reinforced Polyester Matrix Composite in Multilayered Ballistic System, Polymers (Basel). 10 (2018) 230. https://doi.org/10.3390/polym10030230.

7.M. RAMASAMY, A. ARUL DANIEL, M. NITHYA, S. SATHEES KUMAR, R. PUGAZHENTHI, Characterization of natural – Synthetic fiber reinforced epoxy based composite – Hybridization of kenaf fiber and kevlar fiber, Materials Today: Proceedings. 37 (2021) 1699–1705. https://doi.org/10.1016/j.matpr.2020.07.243.

8.S. JAMBARI, M.Y. YAHYA, M.R. ABDULLAH, M. JAWAID, Woven Kenaf/Kevlar Hybrid Yarn as potential fiber reinforced for anti-ballistic composite material, Fibers and Polymers. 18 (2017) 563–568. https://doi.org/10.1007/s12221-017-6950-0.
9.B. DA CRUZ, E.P. LIMA JUNIOR, S.N. MONTEIRO, L.H.L. LOURO, Giant Bamboo Fiber Reinforced Epoxy Composite in Multilayered Ballistic Armor, Materials Research. 18 (2015) 70–75. https://doi.org/10.1590/1516-1439.347514.
10.F.S. DA LUZ, S.N. MONTEIRO, E.S. LIMA, É.P. LIMA JÚNIOR, Ballistic Application of Coir Fiber Reinforced Epoxy Composite in Multilayered Armor, Materials Research. 20 (2017) 23–28 https://doi.org/10.1590/1980-5373-mr-2016-0951.
11.L.A. ROHEN, F.M. MARGEM, S.N. MONTEIRO, C.M.F. VIEIRA, B. MADEIRA DE ARAUJO, E.S. LIMA, Ballistic Efficiency of an Individual Epoxy Composite Reinforced with Sisal Fibers in Multilayered Armor, Materials Research. 18 (2015) 55–62. https://doi.org/10.1590/1516-1439.346314.
12.F.S. DA LUZ, F. DA C. GARCIA FILHO, M.S. OLIVEIRA, L.F.C. NASCIMENTO, S.N. MONTEIRO, Composites with Natural Fibers and Conventional Materials Applied in a Hard Armor: A Comparison, Polymers (Basel). 12 (2020) 1920. https://doi.org/10.3390/polym12091920.
13.P. WAMBUA, B. VANGRIMDE, S. LOMOV, I. VERPOEST, The response of natural fibre composites to ballistic impact by fragment simulating projectiles, Composite Structures. 77 (2007) 232–240. https://doi.org/10.1016/j.compstruct.2005.07.006.
14.M.S. OLIVEIRA, F. DA C.G. FILHO, A.C. PEREIRA, L.F. NUNES, F.S. DA LUZ, F. DE O. BRAGA, H.A. COLORADO, S.N. MONTEIRO, Ballistic performance and statistical evaluation of multilayered armor with epoxy-fique fabric composites using the Weibull analysis, Journal of Materials Research and Technology. 8 (2019) 5899–5908. https://doi.org/10.1016/j.jmrt.2019.09.064.
15.M.S. OLIVEIRA, F. DA C.G. FILHO, F.S. DA LUZ, A.C. PEREIRA, L.C. DA C. DEMOSTHENES, L.F.C. NASCIMENTO, H.A.C. LOPERA, S.N. MONTEIRO, Statistical analysis of notch toughness of epoxy matrix composites reinforced with fique fabric, Journal of Materials Research and Technology. 8 (2019) 6051–6057. https://doi.org/10.1016/j.jmrt.2019.09.079.
16.M. KWIETNIEWSKI, D. MIEDZIŃSKA, Review of Elastomeric Materials for Application to Composites Reinforced by Auxetics Fabrics, Procedia Structural Integrity. 17 (2019) 154–161. https://doi.org/10.1016/j.prostr.2019.08.021.
17.A. KHODADADI, G. LIAGHAT, A.R. BAHRAMIAN, H. AHMADI, Y. ANANI, S. ASEMANI, O. RAZMKHAH, High velocity impact behavior of Kevlar/rubber and Kevlar/epoxy composites: A comparative study, Composite Structures. 216 (2019) 159–167.
https://doi.org/10.1016/j.compstruct.2019.02.080.
18.I.O. OLADELE, T.F. OMOTOSHO, A.A. ADEDIRAN, Polymer-Based Composites: An Indispensable Material for Present and Future Applications, International Journal of Polymer Science. 2020 (2020) 1–12. https://doi.org/10.1155/2020/8834518.
19.U.O. COSTA, L.F.C. NASCIMENTO, J.M. GARCIA, W.B.A. BEZERRA, G.F. FABIO DA COSTA, F.S. DA LUZ, W.A. PINHEIRO, S.N. MONTEIRO, Mechanical properties of composites with graphene oxide functionalization of either epoxy matrix or curaua fiber reinforcement, Journal of Materials Research and Technology. 9 (2020) 13390–13401. https://doi.org/10.1016/j.jmrt.2020.09.035.
20.F. RUBINO, A. NISTICÒ, F. TUCCI, P. CARLONE, Marine Application of Fiber Reinforced Composites: A Review, Journal of Marine Science and Engineering. 8 (2020) 26.
https://doi.org/10.3390/jmse8010026.
21.J.J. ANDREW, S.M. SRINIVASAN, A. AROCKIARAJAN, H.N. DHAKAL, Parameters influencing the impact response of fiber-reinforced polymer matrix composite materials: A critical review, Composite Structures. 224 (2019) 111007. https://doi.org/10.1016/j.compstruct.2019.111007.
22.M.A. ABTEW, F. BOUSSU, P. BRUNIAUX, C. LOGHIN, I. CRISTIAN, Ballistic impact mechanisms – A review on textiles and fibre-reinforced composites impact responses, Composite Structures. 223 (2019) 110966. https://doi.org/10.1016/j.compstruct.2019.110966.

23.K. JHA, R. KUMAR, K. VERMA, B. CHAUDHARY, Y.K. TYAGI, S. SINGH, Application of modified TOPSIS technique in deciding optimal combination for bio-degradable composite, Vacuum. 157 (2018) 259–267. https://doi.org/10.1016/j.vacuum.2018.08.063.
24.M. ALBAWAB, C. GHENAI, M. BETTAYEB, I. JANAJREH, Sustainability Performance Index for Ranking Energy Storage Technologies using Multi-Criteria Decision-Making Model and Hybrid Computational Method, Journal of Energy Storage. 32 (2020) 101820. https://doi.org/10.1016/j.est.2020.101820.
25.O. TAYLAN, D. KAYA, A. DEMIRBAS, An integrated multi attribute decision model for energy efficiency processes in petrochemical industry applying fuzzy set theory, Energy Conversion and Management. 117 (2016) 501–512. https://doi.org/10.1016/j.enconman.2016.03.048.
26.P. CHATTERJEE, N. MANDAL, S. DHAR, S. CHATTERJEE, S. CHAKRABORTY, A novel decision-making approach for light weight environment friendly material selection, Materials Today: Proceedings. 22 (2020) 1460–1469. https://doi.org/10.1016/j.matpr.2020.01.504.
27.P.K. PATNAIK, P.T.R. SWAIN, S.K. MISHRA, A. PUROHIT, S. BISWAS, Composite material selection for structural applications based on AHP-MOORA approach, Materials Today: Proceedings. 33 (2020) 5659–5663. https://doi.org/10.1016/j.matpr.2020.04.063.
28.F.M. AL-OQLA, S.M. SAPUAN, M.R. ISHAK, A.A. NURAINI, Predicting the potential of agro waste fibers for sustainable automotive industry using a decision making model, Computers and Electronics in Agriculture. 113 (2015) 116–127. https://doi.org/10.1016/j.compag.2015.01.011.
29.M. KWIETNIEWSKI, D. MIEDZIŃSKA, Review of Elastomeric Materials for Application to Composites Reinforced by Auxetics Fabrics, Procedia Structural Integrity. 17 (2019) 154–161. https://doi.org/10.1016/j.prostr.2019.08.021.
30.P. CHATTERJEE, N. MANDAL, S. DHAR, S. CHATTERJEE, S. CHAKRABORTY, A novel decision-making approach for light weight environment friendly material selection, Materials Today: Proceedings. 22 (2020) 1460–1469. https://doi.org/10.1016/j.matpr.2020.01.504.
31.Y. SHEN, Y. WANG, Z. YAN, X. CHENG, Q. FAN, F. WANG, C. MIAO, Experimental and Numerical Investigation of the Effect of Projectile Nose Shape on the Deformation and Energy Dissipation Mechanisms of the Ultra-High Molecular Weight Polyethylene (UHMWPE) Composite, Materials. 14 (2021) 4208. https://doi.org/10.3390/ma14154208.
32.B.K. FINK, Performance Metrics for Composite Integral Armor, Journal of Thermoplastic Composite Materials. 13 (2000) 417–431. https://doi.org/10.1106/FR0L-T33W-JPD0-VFH3.
33.L. MOHAMMED, M.N.M. ANSARI, G. PUA, M. JAWAID, M.S. ISLAM, A Review on Natural Fiber Reinforced Polymer Composite and Its Applications, International Journal of Polymer Science. 2015 (2015) 1–15. https://doi.org/10.1155/2015/243947.
34.J.E. MARK, Polymer data handbook., Oxford university press., 2009.
35.M. BREBU, Environmental Degradation of Plastic Composites with Natural Fillers—A Review, Polymers (Basel). 12 (2020) 166. https://doi.org/10.3390/polym12010166.
36.M.A.A. PHILIP M. CUNNIFF, High performance “m5” fiber for ballistics / structural composites, in: n.d.
37.I. BECKMAN, C. LOZANO, E. FREEMAN, G. RIVEROS, Fiber Selection for Reinforced Additive Manufacturing, Polymers (Basel). 13 (2021) 2231. https://doi.org/10.3390/polym13142231.
38.V. MAHESH, S. JOLADARASHI, S.M. KULKARNI, A comprehensive review on material selection for polymer matrix composites subjected to impact load, Defence Technology. 17 (2021) 257–277. https://doi.org/10.1016/j.dt.2020.04.002.
39.H.M. AKIL, M.F. OMAR, A.A.M. MAZUKI, S. SAFIEE, Z.A.M. ISHAK, A. ABU BAKAR, Kenaf fiber reinforced composites: A review, Materials & Design. 32 (2011) 4107–4121. https://doi.org/10.1016/j.matdes.2011.04.008.
40.K.N. KEYA, N.A. KONA, F.A. KOLY, K.M. MARAZ, MD.N. ISLAM, R.A. KHAN, Natural fiber reinforced polymer composites: history, types, advantages, and applications, Materials Engineering Research. 1 (2019) 69–87. https://doi.org/10.25082/MER.2019.02.006.

41.M. LI, Y. PU, V.M. THOMAS, C.G. YOO, S. OZCAN, Y. DENG, K. NELSON, A.J. RAGAUSKAS, Recent advancements of plant-based natural fiber–reinforced composites and their applications, Composites Part B: Engineering. 200 (2020) 108254. https://doi.org/10.1016/j.compositesb.2020.108254.
42.S.R. DJAFARI PETROUDY, Physical and mechanical properties of natural fibers, in: Advanced High Strength Natural Fibre Composites in Construction, Elsevier, 2017: pp. 59–83. https://doi.org/10.1016/B978-0-08-100411-1.00003-0.
43.D.U. SHAH, Natural fibre composites: Comprehensive Ashby-type materials selection charts, Materials & Design (1980-2015). 62 (2014) 21–31. https://doi.org/10.1016/j.matdes.2014.05.002.
44.D.-Y. CHANG, Applications of the extent analysis method on fuzzy AHP, European Journal of Operational Research. 95 (1996) 649–655. https://doi.org/10.1016/0377-2217(95)00300-2.
45.S. RAJU, G.B. MURALI, P.K. PATNAIK, Ranking of Al-CSA composite by MCDM approach using AHP–TOPSIS and MOORA methods, Journal of Reinforced Plastics and Composites. 39 (2020) 721–732. https://doi.org/10.1177/0731684420924833.
46.K. JHA, R. KUMAR, K. VERMA, B. CHAUDHARY, Y.K. TYAGI, S. SINGH, Application of modified TOPSIS technique in deciding optimal combination for bio-degradable composite, Vacuum. 157 (2018) 259–267. https://doi.org/10.1016/j.vacuum.2018.08.063.
47.B. SWAIN, M. PRIYADARSHINI, S.S. MOHAPATRA, R.K. GUPTA, A. BEHERA, Parametric optimization of atmospheric plasma spray coating using fuzzy TOPSIS hybrid technique, Journal of Alloys and Compounds. 867 (2021) 159074. https://doi.org/10.1016/j.jallcom.2021.159074.
48.V. MAHESH, S. JOLADARASHI, S.M. KULKARNI, A comprehensive review on material selection for polymer matrix composites subjected to impact load, Defence Technology. 17 (2021) 257–277. https://doi.org/10.1016/j.dt.2020.04.002.
49.S.N.A. SAFRI, M.T.H. SULTAN, M. JAWAID, K. JAYAKRISHNA, Impact behaviour of hybrid composites for structural applications: A review, Composites Part B: Engineering. 133 (2018) 112–121. https://doi.org/10.1016/j.compositesb.2017.09.008.
50.S. CHOCRON, A.J. CARPENTER, N.L. SCOTT, R.P. BIGGER, K. WARREN, Impact on carbon fiber composite: Ballistic tests, material tests, and computer simulations, International Journal of Impact Engineering. 131 (2019) 39–56. https://doi.org/10.1016/j.ijimpeng.2019.05.002.
51.S. RAJOLE, K.S. RAVISHANKAR, S.M. KULKARNI, Performance study of jute-epoxy composites/sandwiches under normal ballistic impact, Defence Technology. 16 (2020) 947–955. https://doi.org/10.1016/j.dt.2019.11.011.
52.A. HE, G. XIE, H. ZHANG, X. WANG, A comparative study on Johnson–Cook, modified Johnson–Cook and Arrhenius-type constitutive models to predict the high temperature flow stress in 20CrMo alloy steel, Materials & Design (1980-2015). 52 (2013) 677–685. https://doi.org/10.1016/j.matdes.2013.06.010.
53.A. ŠKRLEC, J. KLEMENC, Estimating the Strain-Rate-Dependent Parameters of the Cowper-Symonds and Johnson-Cook Material Models using Taguchi Arrays, Strojniški Vestnik - Journal of Mechanical Engineering. 62 (2016) 220–230. https://doi.org/10.5545/sv-jme.2015.3266.
54.C. HERNANDEZ, A. MARANON, I.A. ASHCROFT, J.P. CASAS-RODRIGUEZ, A computational determination of the Cowper–Symonds parameters from a single Taylor test, Applied Mathematical Modelling. 37 (2013) 4698–4708. https://doi.org/10.1016/j.apm.2012.10.010.
55.M.F. ISMAIL, M.T.H. SULTAN, A. HAMDAN, A.U.M. SHAH, M. JAWAID, Low velocity impact behaviour and post-impact characteristics of kenaf/glass hybrid composites with various weight ratios, Journal of Materials Research and Technology. 8 (2019) 2662–2673. https://doi.org/10.1016/j.jmrt.2019.04.005.
56.J.O. HALLQUIST, LS-DYNA Keyword User's Manual - Version 971., Livermore Software Technology Corporation, Livermore., 2020.

57.V. MAHESH, S. JOLADARASHI, S.M. KULKARNI, Comparative study on kevlar/carbon epoxy face sheets with rubber core sandwich composite for low velocity impact response: FE approach, Materials Today: Proceedings. 44 (2021) 1495–1499. https://doi.org/10.1016/j.matpr.2020.11.688.
58.V. MAHESH, S. JOLADARASHI, S.M. KULKARNI, Damage mechanics and energy absorption capabilities of natural fiber reinforced elastomeric based bio composite for sacrificial structural applications, Defence Technology. 17 (2021) 161–176. https://doi.org/10.1016/j.dt.2020.02.013.
59.V. MAHESH, D. HARURSAMPATH, V. MAHESH, An experimental study on ballistic impact response of jute reinforced polyethylene glycol and nano silica based shear thickening fluid composite, Defence Technology. (2021). https://doi.org/10.1016/j.dt.2021.03.013.
60.V. MAHESH, S. JOLADARASHI, S.M. KULKARNI, Comparative study on energy absorbing behavior of stiff and flexible composites under low velocity impact, in: 2019, p. 020025. https://doi.org/10.1063/1.5085596.

Manuscript received: 26.04.2022